Geochemical and Hydrologic Processes Controlling Formation of Ferricrete

By Laurie Wirt, Kirk R. Vincent, Philip L. Verplanck, Douglas B. Yager, Stanley E. Church, and David L. Fey

Chapter E17 of

Integrated Investigations of Environmental Effects of Historical Mining in the Animas River Watershed, San Juan County, Colorado

Edited by Stanley E. Church, Paul von Guerard, and Susan E. Finger

Professional Paper 1651

U.S. Department of the Interior
U.S. Geological Survey

Contents

Figures

Tables

Chapter E17
Geochemical and Hydrologic Processes Controlling Formation of Ferricrete

By Laurie Wirt, Kirk R. Vincent, Philip L. Verplanck, Douglas B. Yager, Stanley E. Church, and David L. Fey

Abstract

Ferricrete and the acidic water from which it forms provide geochemical baselines of premining conditions in highly mineralized geologic settings. Ferricrete and bog iron deposits composed primarily of goethite, schwertmannite, and amorphous iron oxyhydroxide minerals yield important clues regarding the release of trace elements from weathering of iron sulfides, subsequent transport, and storage in shallow terrestrial and aqueous environments. Goethite and schwertmannite are the two most common iron-oxide minerals present in ferricrete and are commonly saturated in iron-rich ground water. Goethite forms throughout the full range of field pH conditions (pH 2.5 to 7), whereas optimal precipitation of schwertmannite occurs from pH 3 to 4.5, which is analogous to geochemical conditions for acidic mine drainage. Schwertmannite is amorphous and usually converts quickly to goethite, but it may be preserved in some geochemical environments. Radiocarbon dating of wood and charcoal encased in schwertmannite-bearing ferricrete ranges from modern to 9,000 cal. years B.P., indicating that schwertmannite formed in the premining past as well as in the modern postmining period. Preserved prehistorical schwertmannite provides mineralogical evidence for paleo ground-water pH.

Ferricrete forms down gradient from subbasins with large exposures of acid-generating rock types (as much as 60 percent areal extent) containing pyrite and other sulfide minerals. Ferricrete and bog iron form when reduced, acidic ground water discharges near the surface and becomes oxidized. Iron-oxide deposits provide a sink for potentially mobile iron and sulfate, and some trace elements such as zinc, copper, and arsenic that are toxic to aquatic life. We compare acid-sulfate-type ground water from active ferricrete deposits with both mine-affected drainage and ground-water samples from other parts of the watershed using a plot of pH versus the sum of metals. Mine-affected drainage tends to be more acidic and elevated in the concentrations of trace elements such as copper and zinc than acid-sulfate-type water, by as much as two orders of magnitude. Such comparisons can be used as a geochemical baseline for acid-sulfate-type ground water draining hydrothermally altered Tertiary-age volcanic rock in a temperate alpine setting.

Introduction

This chapter focuses on geochemical processes that produce bog iron and ferricrete, describes environmental settings where bog iron and ferricrete form, and compares the water chemistry of non-mining-affected acid drainage and mining-affected acid drainage.

Ferricrete and bog iron deposits are the byproducts of near-surface weathering of iron-sulfide minerals, a natural process that generates acid drainage. Geologists have long known that weathered alpine exposures of mineralized terrains can produce acid drainage (Ransome, 1901; Harder, 1915; Lovering, 1929; Theobald and others, 1963; Hanshaw, 1974). More recently, researchers have recognized that ferricrete and the acidic water from which it forms provide geochemical baselines of premining conditions in highly mineralized geologic settings (Bassett and others, 1992; Furniss and Hinman, 1998; Furniss and others, 1999; Miller and McHugh, 1994; Miller and others, 1999). When reducing iron-rich acidic ground water is exposed to atmosphere or oxygenated surface water, impure iron oxhydroxides precipitate that can take the form of bog iron (stratified iron oxyhydroxide deposits that are relatively clast free) or ferricrete (clastic sedimentary conglomerates cemented by iron oxyhydroxide matrix) as defined by Verplanck and others (this volume, Chapter E15) and Furniss and Hinman (1998). Iron-oxide deposits provide evidence of acid drainage preserved in the geologic record. Until now, however, no watershed-scale investigation of the solid-phase geochemistry of bog iron and ferricrete deposits has taken place that is directly linked to the mineralogy and hydrogeology of the area.

Although natural in origin, many iron-oxide minerals found in bog iron deposits and ferricrete have also been identified in acidic mine drainage. For the following reasons, the study of ferricrete provides a natural analog for such drainage:

1. Ferricrete deposits provide evidence for acidic baseline conditions prior to mining in the area.

2. The geochemical and hydrologic processes involved in ferricrete formation are analogous to those involved in acidic mine drainage, having implications for rates of

transport and storage of iron, sulfate, and potentially toxic base metals such as copper, zinc, arsenic, lead, cadmium, and nickel in a near-surface environment.

3. Ferricrete and bog iron deposits may serve as a solid-phase sink or long-term repository for base metals that pose toxicity to aquatic life if mobile in water.

4. A systematic study of solid-phase chemistry of ferricrete and the ground water from which it forms could be used to develop a site-specific geochemical baseline for "worst-case" ground-water chemistry resulting from the weathering of sulfide mineral deposits.

What is ferricrete? Ferricrete is iron-cemented clastic sediment. Bog iron is a subcategory of ferricrete that consists of stratified, impure iron oxides with relatively few clasts, that have formed in bogs, iron springs, and other shallow wetlands (for a classification of ferricrete categories, see Verplanck and others, this volume; Yager and Bove, this volume, Chapter E1, pl. 2). Bog iron typically has relatively low porosity and forms near the ground surface. Organic debris such as algal filaments, evergreen needles, and branches are common trace fossils replaced by iron oxides in bog deposits. Conglomerate-type ferricrete deposits are dominated by sand and gravel clasts and contain variable amounts of iron cement, thus having variable porosity. They may also contain fossil branches and logs, typically from flood or avalanche debris. Both bog iron and ferricrete conglomerate are abundant in shallow valley fill and along the streambanks of Cement Creek and Mineral Creek in the Animas River watershed study area.

Two conditions are required for the formation of ferricrete. The first is a large, long-term source of dissolved iron, which is generally produced by weathering of hydrothermally altered rock containing pyrite that has little acid-neutralizing capacity. Areas of acid-generating rock types are exposed in the Red Mountains, Ohio Peak–Anvil Mountain, and peak 3,792 m area between Middle and South Forks Mineral Creek (fig. 1). Both the Cement Creek and Mineral Creek basins contain numerous iron springs, iron bogs, and stream-deposited ferricrete that are spatially associated with the hydrothermally altered mineral assemblages in the headwaters and tributary drainages of these basins. Dating of ferricrete in the Animas River watershed study area using ^{14}C methods and age constraints of sediment host deposits indicates a broad age range spanning the late Holocene (Vincent and others, this volume, Chapter E16).

The second condition is when reduced acid-sulfate ground water mixes with oxygen to drive the precipitation of iron minerals. This condition is found in a variety of hydrologic settings in which low-pH and low-Eh ground water comes in contact with the atmosphere or with oxygen generated by bacteria or plants (Stanton, Yager, and others, this volume, Chapter E14) or mixes with shallow oxygenated water. Environmental settings where ferricrete typically forms include iron springs, iron bogs (which are also iron fens), and stream terraces of low-pH streams.

Iron bogs and springs commonly occur where the water table intersects the land surface, frequently at the topographic break in slope along the valley sides. Bog iron is deposited in relatively low gradient wetland environments, generally on flood plains, or superimposed on stream-terrace deposits along the valley floor. In contrast to iron springs and bogs, conglomerate-type ferricrete and manganocrete require a framework of permeable clastic material for the precipitation of iron-oxide cement. Iron- and manganese-rich ground water tends to cement surficial deposits, such as hillslope colluvium, alluvial fans, talus cones, and avalanche debris. Bog iron accumulating in a stream terrace or iron precipitating within a gravel deposit is likely to be protected from erosion. Iron cementation can occur in a wide variety of geomorphic settings, including alluvial, colluvial, and stream settings. The length of time needed for cementation to occur is unknown and is thought to vary considerably with respect to the individual environmental setting.

Purpose and Scope

Chapters E15 and E16 provide a geologic framework for (1) the distribution, classification, and morphology of iron- and manganese-rich deposits (Verplanck and others, this volume), and (2) the surficial geomorphology and relative age of unconsolidated deposits in Cement Creek in relation to the occurrence and distribution of ferricrete (Vincent and others, this volume). In addition, plate 2 in Yager and Bove (this volume) maps the distribution of bog iron and ferricrete deposit types throughout the Animas River watershed study area. The objectives of this chapter are to:

- Describe aqueous-phase geochemistry of acid-sulfate ground water that precipitates iron oxyhydroxides, including pH relations and saturation state of common iron mineral species

- Describe mineralogy, age of host deposits, and solid-phase geochemistry of iron bog deposits, iron-spring deposits, and alluvial and colluvial ferricrete deposits

- Compare major- and trace-element concentrations of iron deposits with those for manganocrete and local stream-deposited sediment

- Characterize spatial relations among acid-generating rock types, ground-water pH, and the occurrence and distribution of iron- and manganese-cemented deposits

- Compare the water chemistry of the acid-sulfate ground water that produces ferricrete with that of mine-affected water to provide a worst-case geochemical baseline of the acid drainage and trace-metal concentrations prior to mining.

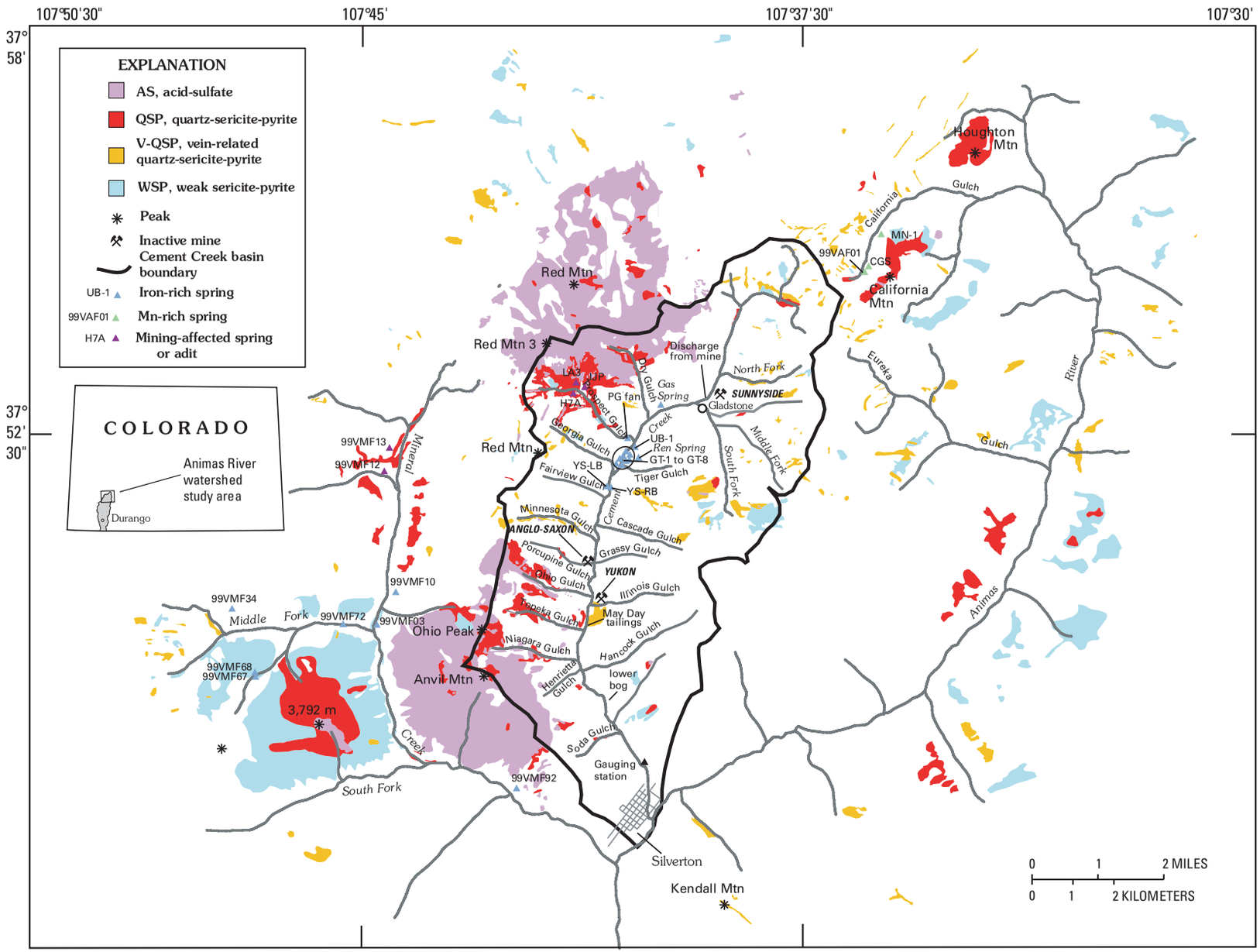

Figure 1. Selected reaches in Cement Creek, Mineral Creek, and California Gulch, major hydrothermal alteration provinces, and water sample localities. Hydrothermal alteration assemblages are from Bove and others (this volume, Chapter E3). Ferricrete deposits in Cement Creek basin were emphasized in this investigation. Water chemistry in table 1.

Methods

Water-Quality Sampling

Water-quality samples were collected from 19 iron-rich springs, 3 manganese-rich springs, and 5 mine-affected sites that appeared to be forming iron oxyhydroxide precipitates, or in a few localities, manganese-oxide precipitates or coatings. Most of these water samples were in contact with fine-grained iron precipitates that were either suspended or settled, and likely contained iron colloids. Every effort was made to collect water samples at the point where the spring emerged from the ground with the greatest flow, in an attempt to collect water before equilibration with atmosphere. In areas of diffuse seepage, we selected the sampling location by surveying with field meters to find areas with the lowest pH and dissolved oxygen. Field parameters including pH, temperature, specific conductance, and dissolved oxygen were measured on site. Each sample was filtered on site using either a small pump with a Gelman 0.45-µm (micrometer) capsule or syringe-mounted 0.45-µm Gelman Acro-disc, and then acidified. One aliquot was acidified with ultrapure hydrochloric acid for analysis of Fe^{+2} speciation and total iron. A separate aliquot was acidified with ultrapure nitric acid to a pH less than 2.0 for analysis of dissolved major and trace elements.

Water-Chemistry Analysis

Filtered, acidified water samples were analyzed for dissolved major and trace cations and sulfate. Major elements were determined by inductively coupled plasma–atomic emission spectrometry (ICP-AES; Briggs and Fey, 1996), and trace elements and sulfate were measured by inductively coupled plasma–mass spectroscopy (ICP-MS; Lamothe and others, 1999). Concentrations of the anions fluoride, chloride, and nitrate were determined by ion chromatography in filtered, unacidified samples (d'Angelo and Ficklin, 1996). Most samples had pH values less than 4.5, and for these samples the presence of bicarbonate as an anion was assumed to be negligible. Four samples in Mineral Creek had pH greater than 4.5, and alkalinity was measured using a HACH titration kit to determine bicarbonate concentration. Analytical detection limits by laboratories used in this study are reported in Lamothe and others (1999) and d'Angelo and Ficklin (1996). In 1999, iron (II) redox species were determined using a modification of the FerroZine™ colorimetric method (Stookey, 1970; To and others, 1999) with a Hewlett Packard 8453™ diode array UV/VIS spectrophotometer. Between 2000 and 2002, the phenanthroline colorimetric method was used (Hach Company, 1992). Water-chemistry data for the ground-water samples is in table 1 and in the project database (Sole and others, this volume, Chapter G).

Solid-Phase Samples

Bog iron and ferricrete samples were collected in concert with the mapping of ferricrete deposits in the Animas River watershed study area (Verplanck and others, this volume; Vincent and others, this volume; Yager and Bove, this volume, pl. 2). We collected representative hand specimens as grab samples, using a rock hammer. Iron-rich solid-phase samples were collected from bog iron deposits, iron springs, and iron-cemented conglomerates containing both alluvial (rounded) rock clasts deposited by fluvial processes and colluvial (angular) rock clasts deposited by hillslope processes. Eighty-six solid-phase samples were analyzed for solid-phase chemistry in this study (tables 2 and 3). These include 26 iron-bog, 15 iron-spring, 21 alluvial-ferricrete, 16 colluvial-ferricrete, and 8 manganocrete samples. In some localities the sample environment was transitional between two or more lithologic facies, but for the purposes of sample coding, a dominant facies was assigned on the basis of the field descriptions. In addition, solid-phase analytical results were compared with 39 premining stream-deposited sediment and 10 modern stream-deposited sediment samples from Cement Creek described by Church, Fey, and Unruh (this volume, Chapter E12). Attributes such as stream reach, deposit type, age of host sediment, and the most abundant iron oxyhydroxide minerals for the solid-phase samples are also given. Chemical analyses and sample descriptions are in the project database (Sole and others, this volume).

Many iron-oxide specimens exhibited a wide color range from yellow to orange brown to reddish brown to brown, representing both crystalline and amorphous iron oxyhydroxide phases. Results from radiocarbon dating and geomorphological constraints for the host deposits indicate a maximum age of ferricrete deposition (table 2), and are further described in Vincent and others (this volume). No credible evidence was found for ferricrete deposits older than the last glacial advance, and we see it as improbable that these surficial deposits would have survived glacial scouring. The samples included both postglacial and modern iron-rich deposits that include bogs, alluvial ferricrete, and colluvial ferricrete deposits.

The majority of the solid-phase samples were collected from the Cement Creek basin because of the nearly continuous occurrence of bog iron deposits and ferricrete in its upper and lower reaches, in particular between the confluence of Cement Creek with the North Fork Cement Creek and Fairview Gulch tributaries (Yager and Bove, this volume, pl. 2). The sample density in the Cement Creek basin allows for spatial correlation with hydrothermal alteration mapping by Bove and others (this volume, Chapter E3), detailed geomorphological mapping by Vincent and others (this volume), and tracer injection and synoptic sampling by Kimball and others (this volume, Chapter E9). Additional iron oxyhydroxide samples were collected along Mineral Creek, and manganocrete samples were collected from the headwaters of the upper Animas River basin in the Eureka and California Gulch subbasins near California Mountain (Yager and Bove, this volume).

Solid-Phase Chemistry Analysis and Mineralogy

Methods for physically separating the solid-phase matrix from the ferricrete and manganocrete samples are described in Verplanck and others (this volume), as are X-ray diffraction techniques for determining the mineralogy of the matrix samples. During sample preparation of ferricrete samples, the iron-rich matrix was separated from the lithic clasts. We dislodged the cement matrix using the rocking motion of a ceramic hammer on the sample. The sample was placed on a ceramic plate and then sifted through an 80-mesh (180-micrometer) sieve. Solid-phase samples were prepared for analysis of major and trace elements using mixed-acid total digestion, followed by inductively coupled plasma–atomic emission spectroscopy (ICP-AES) (Briggs and Fey, 1996). Weight percent of sulfur was analyzed by SGS (Société Génerale de Surveillance) Minerals Laboratories, formerly known as X-Ray Assay Laboratories (XRAL), using high-temperature combustion in a stream of oxygen in the presence of elemental iron. This combustion produces SO_2 gas whose concentration was determined using an infrared detector. Results of analyses for major oxide elements and sulfur (in weight percent; wt. %); trace elements (in parts per million; ppm), and the presence of major iron minerals and rock-forming minerals are reported in the project database (Sole and others, this volume).

Aqueous Geochemistry of Iron-Rich Ground Water

In areas underlain by hydrothermally altered rock with abundant pyrite and poor acid-neutralizing capacity, the pH values of springs and low-flow streams are commonly ≤4.5, and sulfate supplies most of the anionic charge. In areas underlain by propylitically altered rock, calcium is the dominant cation, followed by magnesium and silica. Calcium and magnesium are mostly derived from minerals produced by regional propylitic alteration such as clinochlore chlorite, epidote, calcite, or gypsum, or from sedimentary carbonate rock outside the southeast margin of the caldera (Yager and Bove, this volume, pl. 1). In propylitized areas, calcite in fractures and veins provides a degree of acid neutralization to low-pH waters.

In a steep-gradient alpine environment, water-rock interaction is the primary mechanism that oxidizes and dissolves disseminated pyrite in hydrothermally altered rock and veins. Most of the annual precipitation that falls at higher elevations leaves the watershed as snowmelt and rainfall runoff; however, a fraction of the surface water travels below the water table through saturated soil, talus, and fractured bedrock. Dissolved oxygen is consumed by reactions (1) through (3) following (Kleinman and others, 1981; Bigham and others, 1990), resulting in increasing levels of dissolved iron (Fe^{2+}) and acidity:

$$FeS_2 + 3.5O_2 + H_2O \rightarrow Fe^{2+} + 2H^+ + 2\,SO_4^{2-} \quad (1)$$

$$Fe^{2+} + 0.25O_2 + H^+ \rightarrow Fe^{3+} + 0.5H_2O \quad (2)$$

$$FeS_2 + 14Fe^{3+} + 8\,H_2O \rightarrow 15Fe^{2+} + 2\,SO_4^{2-} + 16\,H^+ \quad (3)$$

Surficial exposures of pyrite-bearing rock (typically unsaturated) produce brightly colored alteration halos of jarosite and hematite, particularly at higher elevations. Bog iron and ferricrete deposits, predominantly found down gradient at lower elevations and in water-saturated environments, are composed mainly of schwertmannite, goethite, and amorphous ferrihydrite. The type of iron oxyhydroxide mineral formed depends on the chemistry and pH of the hydrologic environment and the oxidation state of the iron.

The greater the distribution of iron-sulfide minerals (commonly pyrite), the greater the degree of acidic weathering, and the more likely that undiluted ground water in fractured rock will accumulate H^+, Fe^{+2}, SO_4^{2-}, and trace elements with distance along the flow path. Acidic, anaerobic conditions favor reduced, ferrous (Fe^{+2}) iron. Divalent iron is soluble and thus mobile in ground water. In contrast, more alkaline and aerobic conditions favor formation of oxidized, ferric (Fe^{+3}) iron, which has a lower solubility and low mobility in ground water. At lower pH, iron bacteria promote the precipitation of iron oxyhydroxide minerals in near-surface environments such as bog iron deposits and springs (Stanton, Yager, and others, this volume, Chapter E14). Photoreduction may also play a role in iron oxidation, affecting diurnal rates of iron precipitation. In a small acidic Colorado stream, McKnight and others (1988) reported that daytime oxidation of ferrous iron was almost four times as great as nighttime oxidation of ferrous iron.

In the presence of oxygen, aqueous ferrous iron is converted to ferric iron (precipitate) according to the following reaction (Kleinman and others, 1981; Bigham and others, 1990):

$$Fe^{2+} + 2.5H_2O + 0.25O_2 \rightarrow Fe(OH)_{3(s)} + 2H^+ \quad (4)$$

Ground water emerging from wet ferricrete was sampled from 19 locations where iron oxyhydroxide appeared to be actively forming. Half these sites were in upper Cement Creek, and the remainder in Mineral Creek. Results for major dissolved cations and selected trace elements are in table 1. Three manganese seeps from California Gulch and drainage from three mine adits in Prospect Gulch and two mine-affected springs in Mineral Creek were also sampled. Sampling occurred during low-flow conditions in August to September 1999–2002, and thus year-to-year seasonal variations in water chemistry cannot be determined.

In upper Cement Creek, the pH of iron-rich ground-water samples ranged from 3.0 to 4.6. The pH of ground-water samples in Mineral Creek tended to be higher than in Cement Creek, with all but one pH value ranging between 4.0 and 6.6. The lowest pH value of 2.5 was measured at a mine adit in Prospect Gulch. The pH of manganese-rich water in California Gulch ranged between 4.5 and 4.8. Dissolved oxygen values ranged between 0.01 and 4.4, indicating that the ground water had not yet fully equilibrated with atmosphere.

Table 1. Chemical analyses of water samples collected in contact with iron and manganese precipitates in the Animas River watershed study area.

[Dissolved chemistry for major and trace elements by ICP-AES, except for bold values by ICP-MS. Anion concentrations (chloride, fluoride, and sulfate) by ion chromatography (IC), except as noted. Sample values are in milligrams per liter except for specific conductance (SC), in microsiemens per centimeter; temperature (T), in degrees Celsius; dissolved oxygen (DO); <, less than; ND, not determined]

Sample ID	Reach	Date	SC	pH	T	DO	Ca	Mg	Na	K	Al	Sr	Mn	Cl	F	SO_4
Iron-rich springs																
99VMF10*	Mineral Cr	8/15/1999	1,070	6.6	6.6	ND	250	6.9	10.5	0.85	<0.01	1.97	1.48	2.1	0.6	560
99VMF34	Mineral Cr	8/24/1999	19	5.8	13.9	ND	2.0	0.34	1.7	0.26	0.2	0.02	<0.001	1.8	<0.1	4
99VMF67	Mineral Cr	8/24/1999	127	4.2	2.3	ND	11	1.8	3.9	0.43	0.9	0.10	0.23	1.9	0.2	42
99VMF68	Mineral Cr	8/24/1999	130	4.0	4.1	ND	11	2.0	4.1	0.46	0.9	0.10	0.28	1.9	0.3	44
99VMF92	Mineral Cr	9/1/1999	305	4.4	9.0	ND	24	2.7	3.9	1.4	0.9	0.21	0.20	2.3	0.3	84
99VMF72	Mineral Cr	8/25/1999	341	3.3	6.6	ND	28	3.2	3.8	1.2	2.7	0.20	0.36	4.6	0.3	110
00VMF01	Mineral Cr	9/6/2000	473	4.3	3.5	ND	34	6.2	4.6	0.58	7	0.29	0.66	0.8	0.57	220
00VMF03	Mineral Cr	8/31/2000	777	4.1	8.7	ND	130	4.5	7.1	0.51	1.2	1.30	0.30	0.8	0.23	381
PG fan	U.Cement Cr	8/19/2002	579	3.3	10.9	2.7	24	7.5	1.5	3.9	**16**	0.29	0.69	0.4	0.7	240
YS-LB	U.Cement Cr	10/25/2000	734	3.5	5.3	0.9	75	4.9	2.7	1.0	4.1	0.56	0.58	2.7	0.9	250
YS-RB	U.Cement Cr	10/25/2000	1,219	3.2	7.1	0.3	180	8.4	5.4	2.0	5.1	1.10	1.40	0.6	1.6	630
Gas Spring	U.Cement Cr	8/23/2002	568	4.2	7.1	0.1	50	8.1	2.8	2.9	**9**	0.57	1.10	0.6	0.9	250
Ren Spg	U.Cement Cr	8/23/2002	922	3.6	7.9	0.3	120	7.4	5.2	2.0	12	0.54	0.67	0.6	1.4	430
UB-1	U.Cement Cr	10/25/2000	1,468	3.2	18.5	4.4	210	11	2.6	3.0	13	1.70	1.90	0.6	1.7	760
GT-1	U.Cement Cr	9/24/1999	1,172	3.2	12.2	8.2	180	17	4.9	1.6	9.0	0.83	4.00	2.2	1.0	560
GT-2	U.Cement Cr	9/27/1999	1,613	3.0	10.8	1.2	270	11	4.7	2.1	8.3	1.20	1.80	2.2	1.2	820
GT-3	U.Cement Cr	9/27/1999	1,462	4.6	13.1	0.0	280	11	5.3	2.4	6.1	1.40	2.00	0.6	1.5	780
GT-4	U.Cement Cr	9/27/1999	1,801	3.8	13.6	0.4	330	12	5.4	2.5	7.7	1.50	2.20	2.1	1.3	1,000
GT-7	U.Cement Cr	9/27/1999	1,578	3.3	16.4	4.1	290	11	5.0	2.1	6.2	1.40	1.90	2.1	1.2	790
GT-8	U.Cement Cr	9/27/1999	523	3.6	12.6	4.4	65	6.5	2.8	1.5	2.8	0.41	1.70	0.5	0.5	220
Manganese-rich springs																
99VAF01	California Gulch	8/5/1999	703	4.5	2.6	ND	55.9	9.3	3.2	1.9	24	0.08	57	2.1	30	360
MN-1	California Gulch	10/25/2000	856	4.8	1.8	7.9	44	21	2.2	1.6	24	0.07	48	0.4	3.8	**470**
CGS	California Gulch	8/21/2002	390	4.5	2.9	<4.5	28	3.7	3.0	1.7	**14**	0.04	28	0.3	15	150
Mining-affected springs or adits																
L3A (adit)	Prospect Gulch	9/29/1999	228	4.1	1.1	3.3	16	0.9	2.6	2.2	4.0	0.13	0.22	0.4	0.1	83
JJP (adit)	Prospect Gulch	9/29/1999	1,010	2.7	3.2	7.5	2.7	1.6	0.4	1.6	13	0.05	0.19	0.5	0.4	290
H7A (adit)	Prospect Gulch	9/29/1999	2,450	2.5	2.0	3.6	49	7.5	0.8	1.4	23	0.27	0.91	0.7	1.3	1,100
99VMF13	Mineral Cr	8/23/1999	481	5.8	5.5	ND	66	6.8	6.1	0.68	0.9	0.56	2.46	3.8	1.4	220
99VMF12	Mineral Cr	8/23/1999	344	5.6	4.3	ND	47	3.4	5.7	0.49	0.4	0.29	0.90	3.8	0.7	140

*Possibly mining affected.

Fe	Si	Zn	Cu	Ni	Co	Zn+Cu+Ni+Co	Fe(II)	Fe(III)	Remarks or methods
					Iron-rich springs				
6.8	15	0.026	<0.010	<0.010	0.010	0.036	**6.91**	**6.9**	**Samples run by FerroZine method for iron total and iron II**
0.1	4.8	<.001	<0.010	<0.010	<0.010	0.000	**0.051**	**<0.05**	**Samples run by FerroZine method for iron total and iron II**
<0.02	13.4	<.001	<0.010	<0.010	<0.010	0.000	**<0.01**	**<0.01**	**Samples run by FerroZine method for iron total and iron II**
<0.02	14.8	0.012	<0.010	<0.010	<0.010	0.012	**<0.01**	**<0.01**	**Samples run by FerroZine method for iron total and iron II**
5.8	16	0.021	<0.010	<0.010	<0.010	0.021	**8.4**	**8.0**	**Samples run by FerroZine method for iron total and iron II**
1.1	15	0.037	<0.010	<0.010	<0.010	0.037	**1.2**	**0.3**	**Samples run by FerroZine method for iron total and iron II**
31	26	0.120	0.002	0.007	0.019	0.148	**30.2**	**0.5**	**ICP-MS**
4.7	12.2	0.150	0.002	0.005	0.008	0.165	**4.2**	**0.5**	**ICP-MS**
56	26	**0.677**	**0.027**	**0.021**	**0.025**	0.750	38.1	18.1	bold = ICP-MS HACH for Fe (III)
11	8	0.220	<0.010	0.012	0.019	0.251	20.0	11	**Phenanthroline Chemettes for Fe (II)**
29	12	0.500	0.150	0.020	0.030	0.700	20.0	9.0	**Phenanthroline Chemettes for Fe (II)**
39	26	**0.467**	**0.011**	**0.010**	**0.015**	0.503	5.3	33.6	bold = ICP-MS HACH for Fe (III)
28	22	**0.127**	**0.004**	**0.011**	**0.012**	0.154	12.6	15.5	bold = ICP-MS HACH for Fe (III)
45	12	1.500	<0.010	0.038	0.050	1.588	20.0	45	**Phenanthroline Chemettes for Fe (II)**
0.34	23	0.990	0.080	0.024	0.038	1.132	**0.15**	**0.29**	**Samples run by FerroZine method for iron total and iron II**
20	20	0.780	<0.010	0.025	0.031	0.836	**16.7**	**9.3**	**Samples run by FerroZine method for iron total and iron II**
39	20	0.780	<0.010	0.027	0.035	0.842	**43.0**	**0.0**	**Samples run by FerroZine method for iron total and iron II**
50	21	0.930	<0.010	0.033	0.036	0.999	**66.7**	**0.7**	**Samples run by FerroZine method for iron total and iron II**
28	19	0.790	<0.010	0.027	0.029	0.846	**22.7**	**12.2**	**Samples run by FerroZine method for iron total and iron II**
0.30	15	0.440	0.041	0.010	0.017	0.508	**0.32**	**0.00**	**Samples run by FerroZine method for iron total and iron II**
					Manganese-rich springs				
<0.02	8.7	4.040	<0.010	0.022	<0.010	4.062	**<0.01**	**<0.01**	**Samples run by FerroZine method for iron total and iron II**
0.5	9.3	**14.0**	0.140	0.0120	0.013	14.165	0.10	0.37	
30.4	8.5	**1.74**	**4.60**	**0.0072**	**0.002**	6.349	0.18	30.22	bold = ICP-MS HACH for Fe (III)
					Mining-affected springs or adits				
23	8.1	2.20	0.160	0.0110	0.010	2.381	**22.2**	0.40	
62	27	11.0	0.640	0.0280	0.039	11.707	**0.412**	61.59	
291	6.7	8.2	0.590	0.1100	0.170	9.070	**23.0**	268.00	
12	14.5	0.401	<0.010	<0.010	0.024	0.425	**11.7**	**11.6**	**Samples run by FerroZine method for iron total and iron II**
6.0	14.1	0.114	<0.010	<0.010	0.019	0.114	**5.84**	**5.8**	**Samples run by FerroZine method for iron total and iron II**

Table 2. Summary of solid-phase sample attributes, including reach, deposit type, age of host sediments, and dominant iron mineralogy.

Field No.	Latitude N. (degrees)	Longitude W. (degrees)	Reach	Deposit type	Wet/Dry	Dominant iron mineral[1]	Geomorphologic unit[2] (Vincent and others, this volume)	Age range of host deposit (per 1,000 years)	Site description	Munsell Color code (Goddard and others, 1948)
00ABFC-231	37.879650	107.674545	Upper Cement	Alluvial ferricrete	alluvial	1	p	0.5 to 0	Alluvial ferricrete forming in streambed at upper bog, clasts subrounded, lots of algae growing on cement (from Cement Creek above Georgia Gulch, in streambed).	*7.5YR-4/6* strong brown
99ABFC-102A	37.889351	107.668389	Upper Cement	Alluvial ferricrete	spring	1	T	6 to 0.5	Laminar iron springs deposit overlying alluvial ferricrete, 5 ft above low-flow water level, sample collected from north bank of Cement Creek above confluence with Dry Gulch.	*5YR-3/4* dk reddish brown
99ABFC-108	37.879650	107.668333	Upper Cement	Alluvial ferricrete	alluvial	2	bed	.5 to 0	Alluvial ferricrete forming in streambed at upper bog, clasts subrounded, lots of algae growing on cement (from Cement Creek above Georgia Gulch, in streambed).	*5YR-4/6* yellowish red
99ABFC-110	37.888660	107.668159	Upper Cement	Alluvial ferricrete	dry	2	F or T	10 to .5	Alluvial ferricrete, clasts 6–8 in. down to fine sand, subrounded to subangular, poorly sorted, 2 ft above low-flow water level, sample from south bank Cement Creek below confluence with South Fork Cement Creek.	*7.5YR-4/6* strong brown
99ABFC-111	37.888386	107.656769	Upper Cement	Alluvial ferricrete	dry	2	Fo or T	10 to .5	Alluvial ferricrete, clasts 6–8 in. down to fine sand, subrounded to subangular, moderately sorted, 1 ft above low-flow water level, sample from Cement Creek above confluence with Dry Gulch.	*10YR-3/6* dk yellowish brown
99ABFC-118B	37.883068	107.650864	Upper Cement	Alluvial ferricrete	dry	2	T or p	6 to 0	Alluvial ferricrete, clasts 1–1.5 in. down to fine sand, well sorted, sample from Cement Creek downstream from Dry Gulch confluence.	*5YR-4/6* yellowish red
99ABFC-119	37.882576	107.668800	Upper Cement	Alluvial ferricrete	dry	2	T	6 to .5	Alluvial ferricrete, clasts 3 in. down to fine sand, moderately sorted, 6 ft above low-flow water level, sample from Cement Creek downstream from Dry Gulch confluence.	*10YR-4/6* dk yellowish brown
99ABFC-120	37.882236	107.675308	Upper Cement	Alluvial ferricrete	dry	2	Fy	6 to 0	Alluvial ferricrete, clasts 12 in. down to sand, subangular, poorly sorted, 2 ft above low-flow water level, sample from Cement Creek just downstream from Prospect Gulch confluence.	*10YR-5/8* yellowish brown
99ABFC-124A	37.877666	107.666283	Upper Cement	Alluvial ferricrete	alluvial	2	bed	.5 to 0	Actively forming ferricrete matrix forming on bed of Cement Creek at Tiger Gulch.	*7.5YR-5/8* strong brown

Field No.	Latitude N. (degrees)	Longitude W. (degrees)	Reach	Deposit type	Wet/Dry	Dominant iron mineral[1]	Geomorphologic unit[2] (Vincent and others, this volume)	Age range of host deposit (per 1,000 years)	Site description	Munsell Color code (Goddard and others, 1948)
99ABFC-128A	37.856407	107.667870	Middle Cement	Alluvial ferricrete	dry	2	T	6 to 0.5	Alluvial ferricrete, clasts 6 in. down to fine sand, subrounded, moderately sorted, sample from east bank of Cement Creek below confluence with Porcupine Gulch.	*5YR-3/4* dk reddish brown
99ABFC-128B	37.856407	107.667870	Middle Cement	Alluvial ferricrete	spring	2	T	6 to .5	Iron spring deposit, fine-grained hydrous iron oxides overlying sample 99ABFC-128A.	*7.5YR-3/4* dk brown
99ABFC-136A	37.835297	107.675392	Middle Cement	Alluvial ferricrete	dry	2	T or p	6 to 0	Alluvial ferricrete, clasts 8 in. down to sand, subrounded, moderately sorted, 1 ft above low-flow water level, from unnamed tributary on east side of Cement Creek above Hancock Gulch confluence.	*10YR-4/6* dk yellowish brown
99ABFC-138	37.833183	107.675316	Lower Cement	Alluvial ferricrete	dry	2	T	6 to .5	Alluvial ferricrete, clast size 8 in. to sand, subrounded, moderately sorted, sample from west bank of Cement Creek below confluence with Hancock Gulch.	*7.5YR-4/6* strong brown
99ABFC-141C	37.823231	107.675743	Lower Cement	Alluvial ferricrete	dry	2	Tg	10 to 6	Ferricrete, clasts 2 in. to sand, sub-rounded, moderately sorted.	*7.5YR-4/6* strong brown
99ABFC-151	37.859333	107.677597	Middle Cement	Alluvial ferricrete	dry	2	T?	6 to .5	Alluvial ferricrete, clast size 10 in. to fine sand, subangular, moderately sorted, sample from west bank Cement Creek above confluence with Porcupine Gulch.	*10YR-4/6* dk yellowish brown
99ABFC-154D	37.878017	107.676430	Upper Cement	Alluvial ferricrete	alluvial	5	p	.5 to 0	Alluvial ferricrete, clast size 6 in. to fine sand, subrounded, moderately sorted.	*7.5YR-3/4* dk brown
99ABFC-155	37.889320	107.672768	Upper Cement	Alluvial ferricrete	alluvial	2	p	.5 to 0	Alluvial ferricrete, clasts 6 in. down to fine sand, subangular to subrounded, poorly to moderately sorted, sample from Cement Creek below confluence with South Fork Cement Creek.	*7.5YR-4/6* strong brown
99ABFC-176A	37.895859	107.645218	Upper Cement	Alluvial ferricrete	dry	5	T	2.2 to 0	Alluvial ferricrete, clasts 1 ft down to sand, subangular, moderately sorted, grades vertically into bog iron deposit, sample from Cement Creek above confluence with South Fork Cement Creek.	*7.5YR-4/6* strong brown
99VMS-29	37.860157	107.705559	Mineral Cr	Alluvial ferricrete	dry	2	-	-	Red/brown matrix from ferricrete out-crop, Browns Gulch.	no data
99VMS-33	37.844917	107.725212	Mineral Cr	Alluvial ferricrete	dry	5	-	-	Brown matrix from 100 ft high ferricrete outcrop, Middle Fork Mineral Creek.	*5YR-3/3* and 3/4 dark reddish brown

Table 2. Summary of solid-phase sample attributes, including reach, deposit type, age of host sediments, and dominant iron mineralogy.—Continued

Field No.	Latitude N. (degrees)	Longitude W. (degrees)	Reach	Deposit type	Wet/Dry	Dominant iron mineral[1]	Geomorphologic unit[2] (Vincent and others, this volume)	Age range of host deposit (per 1,000 years)	Site description	Munsell Color code (Goddard and others, 1948)
ODY99-09	37.844189	107.669304	Mineral Cr	Alluvial ferricrete	dry	2	-	-	Alluvial ferricrete deposit consists of subangular to subrounded cobbles with some boulder-size clasts in a granular, iron-cemented matrix (along Middle Fork Mineral Creek).	*7.5YR-4/6* strong brown
99ABFC-115	37.886402	107.656769	Upper Cement	Colluvial ferricretes	dry	2	Fo or P	10 to 0		*7.5YR-4/4* brown
99ABFC-131	37.851616	107.667870	Middle Cement	Colluvial ferricretes	dry	5	F	10 to 0	Ferricrete, large boulders to sand, angular to subrounded clasts, poorly sorted, sample from Cement Cr immediately below Ohio Gulch.	*7.5YR-4/6* strong brown
99ABFC-133	37.850750	107.668449	Middle Cement	Colluvial ferricretes	dry	2	F	10 to 0	Ferricrete, angular clasts from Illinois Gulch, 1 ft to sand, poorly sorted, below Yukon tunnel.	*7.5YR-4/6* strong brown
99ABFC-134	37.845634	107.669815	Middle Cement	Colluvial ferricretes	dry	2	Fo	10 to 6	Ferricrete, clasts 1 ft to sand, mostly subrounded, sample from old Topeka Gulch fan.	*5YR-4/6* yellowish red
99ABFC-153	37.873817	107.677628	Upper Cement	Colluvial ferricretes	dry	2	T?	6 to .5	Alluvial ferricrete, clast size 3 in. to fine sand, subrounded, moderately sorted, grades upward into deposit angular and poorly sorted clasts, sample from Cement Creek above confluence with Fairview Gulch.	*10YR-4/6* dk yellowish brown
99ABFC-170	37.909893	107.650520	Upper Cement	Colluvial ferricretes	dry	2	colluvium	10 to 0	Colluvial ferricrete from above entrance to Mogul mine, fine-grained matrix sampled.	*5YR-4/6* yellowish red
99ABFC-175B	37.902031	107.649010	Upper Cement	Colluvial ferricretes	colluvial	2	T or p	6 to 0	Colluvial ferricrete, manganese-rich hydrous iron oxide, east side of Cement Creek just above Red and Bonita mine.	no data
99ABFC-185C	37.864086	107.643883	Upper Cement	Colluvial ferricretes	dry	2	colluvium	10 to .5	Ferricrete, clasts 1 ft down to sand, angular to subangular, poorly sorted, grades vertically into bog iron deposit, sample from Dry Gulch.	*7.5YR-4/6* strong brown
99VMS-09	37.823612	107.643753	Mineral Cr	Colluvial ferricretes	dry	2	-	-	Matrix from Zuni Gulch angular ferricrete, sample of float.	*5YR 4/6* yellowish red
99VMS-12	37.862469	107.646286	Mineral Cr	Colluvial ferricretes	colluvial	5	-	-	Matrix from ferricrete in outcrop above Imogene mine.	*10R-3/2* dusty red
ODY98-31B	37.833069	107.615082	Mineral Cr	Colluvial ferricretes	spring	5	-	-	Colluvial ferricrete deposit consists of angular to subangular pebble-size clasts in a granular iron oxide cemented matrix (near active iron spring, along north-draining tributary to Middle Fork Mineral Creek).	*7.5YR-4/4* brown

Field No.	Latitude N. (degrees)	Longitude W. (degrees)	Reach	Deposit type	Wet/Dry	Dominant iron mineral[1]	Geomorphologic unit[2] (Vincent and others, this volume)	Age range of host deposit (per 1,000 years)	Site description	Munsell Color code (Goddard and others, 1948)
ODY98-32b	37.833076	107.612541	Mineral Cr	Colluvial ferricretes	spring	5	-	-	Middle of 8-in. long core in active iron spring consists of angular pebble-size clasts in a sand-size light-reddish-brown matrix (north-draining tributary to Middle Fork Mineral Creek).	*5YR-4/6* yellowish red
SDY00-17A2	37.849567	107.753159	Middle Cement	Colluvial ferricretes	dry	2	colluvium	10 to 0	Colluvial ferricrete deposit consists of angular to subangular cobbles and pebbles, some boulder-size clasts in a granular iron oxide cemented matrix (sampled above SDY00-17A1 in Topeka Gulch).	no data
SDY00-2	37.840351	107.758644	Middle Cement	Colluvial ferricretes	dry	2	colluvium	10 to 0	Colluvial ferricrete deposit consists of angular cobbles cemented by a finely layered iron oxide cement, sampled near Niagara Gulch.	*7.5YR-4/6* strong brown
SDY00-28	37.834534	107.758644	Mineral Cr	Colluvial ferricretes	dry	5	-	-	Colluvial ferricrete deposit consists of subangular to subrounded pebbles and cobbles, with several boulder-size clasts in a granular, iron-cemented matrix (west of and above Mineral Creek between Middle and South Fork confluences).	*7.5YR-5/8* strong brown
SDY99-14	37.841110	107.688698	Mineral Cr	Colluvial ferricretes	dry	2	-	-	Colluvial ferricrete deposit consists of subangular to subrounded pebbles and cobbles, some boulder-size clasts in a granular, iron-cemented matrix (sampled on river right bank near northerly draining tributary to Middle Fork Mineral Creek).	*10YR-4/6* dk yellowish brown
99ABFC-122C1	37.880260	107.658249	Upper Cement	Iron bog	bog	1	T or p?	4 to 0	Iron bog, fine-grained hydrous iron oxides, east side Cement Creek below confluence with Prospect Gulch (sample dried before mineralogical analysis).	*2.5YR-4/6* red
99ABFC-122D1	37.880260	107.662880	Upper Cement	Iron bog	bog	1	T	4 to .5	Iron bog, fine-grained hydrous iron oxides, west side Cement Creek above upper bog (sample dried before mineralogical analysis).	*7.5YR-5/6* strong brown
99ABFC-126	37.865639	107.666283	Middle Cement	Iron bog	dry	2	Fy	6 to 0	Iron bog deposit, fine-grained iron oxides, sample from west bank of Cement Creek above confluence with Minnesota Gulch in alluvial fan.	*5YR-3/4* dk reddish brown
99ABFC-141B	37.823231	107.676201	Lower Cement	Iron bog	dry	1	Tg	4.5	Bog iron, fine-grained hydrous iron oxides at top of thick ferricrete section, sample from road cut on east side Cement Creek just above Silverton.	*7.5YR-4/6* strong brown

Table 2. Summary of solid-phase sample attributes, including reach, deposit type, age of host sediments, and dominant iron mineralogy.—Continued

Field No.	Latitude N. (degrees)	Longitude W. (degrees)	Reach	Deposit type	Wet/Dry	Dominant iron mineral[1]	Geomorphologic unit[2] (Vincent and others, this volume)	Age range of host deposit (per 1,000 years)	Site description	Munsell Color code (Goddard and others, 1948)
99ABFC-161	37.883244	107.669373	Upper Cement	Iron bog	dry	2	bog on T or p	6 to 0	Bog iron deposit, fine-grained iron oxides, sample from South Fork Cement Creek.	*5YR-3/4* dk reddish brown
99ABFC-162A	37.869652	107.669373	Upper Cement	Iron bog	dry	1	bog on T or p	6 to 0	Bog iron deposit, fine-grained iron oxides, sample from head of South Fork Cement Creek.	*5YR-3/4* dk reddish brown
99ABFC-173	37.904663	107.650108	Upper Cement	Iron bog	dry	2	T or p	6 to 0	Bog iron deposit, fine-grained hydrous iron oxides, west side of Cement Creek downstream from Mogul mine.	*5YR-4/6* yellowish red
99ABFC-176B	37.895859	107.644287	Upper Cement	Iron bog	dry	2	T	2.2 to 0	Bog iron deposit, fine-grained iron oxides with wood fragments.	*2.5YR-4/6* dk red
99VMS-14	37.870556	107.611313	Mineral Cr	Iron bog	mine	1	-	-	Ferricrete soil from hillside above (west side) Chattanooga beaver ponds.	*5YR-4/6* yellowish red
99VMS-92	37.816113	107.725830	Mineral Cr	Iron bog	bog	1	-	-	Iron bog area along Mineral Creek below Columbine mine.	*5YR-3/3* dk reddish brown
IDY00-14	37.894455	107.726669	Upper Cement	Iron bog	dry	1	?	10 to 0	Bog iron deposit consists entirely of iron oxide matrix with finely layered texture (near mouth of North Fork Cement Creek).	*7.5YR-4/6* strong brown
IDY00-29A	37.883202	107.697220	Upper Cement	Iron bog	dry	1	colluvium?	10 to 0	Banded bog iron deposit consists of alternating 3 mm to 10 mm thick iron oxide matrix layers, dark-brown bands in hand sample (near lower Prospect Gulch spring).	*5YR-4/6* yellowish red
IDY00-29B	37.883202	107.566333	Upper Cement	Iron bog	dry	1	colluvium?	10 to 0	Banded bog iron deposit consists of alternating 3 mm to 10 mm thick iron oxide matrix layers, yellow bands in hand sample (near lower Prospect Gulch spring).	*10YR-5/8* yellowish brown
SDY00-17A1	37.849567	107.669304	Middle Cement	Iron bog	dry	2	colluvium	10 to 0	Bog iron deposit consists entirely of iron oxide matrix with finely layered texture (sample from Topeka Gulch).	*7.5YR-3/4* dk brown
95-ABS-117	37.879667	107.671776	Upper Cement	Iron bog	bog	1	T or p	6 to 0	Upper iron bog, Cement Creek (total digestion analysis).	no data
95-ABS-119	37.897034	107.612030	Upper Cement	Iron bog	dry	2	?	10 to 0	Bog iron deposit exposed on upper Cement Creek below Red and Bonita mine (partial digestion analysis).	no data
97ABS-318a	37.816307	107.668800	Mineral Cr	Iron bog	bog	1	-	-	Fine-grained iron bog deposit, depth 1.25 in. below surface, north bank South Fork Mineral Creek.	*2.5YR-3/4* dk reddish brown
97ABS-318b	37.816307	107.675377	Mineral Cr	Iron bog	bog	1	-	-	Fine-grained iron bog deposit, depth 4.75 in. below surface, north bank of South Fork Mineral Creek.	*5YR-4/6* yellowish red
97ABS-318c	37.816307	107.736839	Mineral Cr	Iron bog	bog	1	-	-	Fine-grained iron bog deposit, depth 7.25 in. below surface, north bank South Fork Mineral Creek.	*2.5YR-2.5/4* dk reddish brown
97ABS-323a	37.879667	107.729752	Upper Cement	Iron bog	bog	1	T or p	6 to 0	Fine-grained iron bog deposit, depth 0.5 in., west bank of Cement Creek, upper bog below confluence with Prospect Gulch.	*5YR-4/6* yellowish red

Field No.	Latitude N. (degrees)	Longitude W. (degrees)	Reach	Deposit type	Wet/Dry	Dominant iron mineral[1]	Geomorphologic unit[2] (Vincent and others, this volume)	Age range of host deposit (per 1,000 years)	Site description	Munsell Color code (Goddard and others, 1948)
97ABS-323b	37.879667	107.729752	Upper Cement	Iron bog	bog	1	T or p	6 to 0	Fine-grained iron bog deposit, depth 4.25 in., west bank of Cement Creek upper bog below confluence with Prospect Gulch.	*2.5YR-2.5/4* dk reddish brown
97ABS-323c	37.879667	107.729752	Upper Cement	Iron bog	bog	1	T or p	6 to 0	Fine-grained iron bog deposit, depth 6.75 in., west bank of Cement Creek upper bog below confluence with Prospect Gulch.	*5YR-4/6* yellowish red
97ABS-325a	37.879667	107.729752	Upper Cement	Iron bog	bog	1	T or p	6 to 0	Fine-grained iron bog deposit, depth 2 in., east bank of Cement Creek upper bog below confluence with Prospect Gulch.	*5YR-4/6* yellowish red
97ABS-325b	37.879667	107.729752	Upper Cement	Iron bog	bog	1	T or p	6 to 0	Fine-grained iron bog deposit, depth 4 in., east bank of Cement Creek upper bog below confluence with Prospect Gulch.	*5YR-4/6* yellowish red
97ABS-325c	37.879667	107.736639	Upper Cement	Iron bog	bog	1	T or p	6 to 0	Fine-grained iron bog deposit, depth 11.75 in., east bank of Cement Creek upper bog below confluence with Prospect Gulch.	*5YR-4/6* yellowish red
97ABS-325d	37.879667	107.736444	Upper Cement	Iron bog	bog	1	T or p	6 to 0	Fine-grained iron bog deposit, depth 11 in., east bank of Cement Creek upper bog below confluence with Prospect Gulch.	*5YR-4/6* yellowish red
99ABFC-102B	37.889351	107.668333	Upper Cement	Iron spring	dry	2	T or p	6 to 0	Laminar iron springs deposit overlying alluvial ferricrete, 1.5 ft above low-flow water level, sample collected from north bank of Cement Creek above confluence with Dry Gulch.	*5YR-4/6* yellowish red
99ABFC-139	37.831554	107.675316	Lower Cement	Iron spring	dry	2	T or p	6 to 0	Iron spring deposit, fine-grained hydrous iron oxides, sample from east bank of Cement Creek above confluence with Soda Gulch.	*7.5YR-4/6* strong brown
99ABFC-146A	37.883030	107.676003	Upper Cement	Iron spring	spring	1	Fo	10 to 6	Iron spring deposit, fine-grained hydrous iron oxides from lower spring on Prospect Gulch.	*7.5YR-3/4* dk brown
99ABFC-154A1	37.878017	107.673035	Upper Cement	Iron spring	spring	1	p	.5 to 0	Iron spring deposit, laminated iron oxides in dormant mound, east side of Cement Creek above confluence with Tiger Gulch.	*2.5YR-3/6* dk red
99ABFC-154A2	37.878017	107.671127	Upper Cement	Iron spring	spring	1	p	.5 to 0	Iron spring deposit, active at base.	no data
99ABFC-154B1	37.878017	107.664719	Upper Cement	Iron spring	spring	1	p	.5 to 0	Iron springs deposit,1 ft above low-flow water level, east side of Cement Creek (sample dried prior to mineralogical analysis).	*5YR-4/6* yellowish red
99ABFC-154B2	37.878017	107.664719	Upper Cement	Iron spring	spring	1	p	.5 to 0	Iron springs deposit,1 ft above low-flow water level, east side of Cement Creek (wet sample preserved for mineralogical analysis).	no data

Table 2. Summary of solid-phase sample attributes, including reach, deposit type, age of host sediments, and dominant iron mineralogy.—Continued

Field No.	Latitude N. (degrees)	Longitude W. (degrees)	Reach	Deposit type	Wet/Dry	Dominant iron mineral[1]	Geomorphologic unit[2] (Vincent and others, this volume)	Age range of host deposit (per 1,000 years)	Site description	Munsell Color code (Goddard and others, 1948)
99ABFC-154C	37.878017	107.666595	Upper Cement	Iron spring	spring	5	p	.5 to 0	Iron springs deposit, 1 ft above low-flow water level, west side of Cement Creek.	*7.5YR-4/6* strong brown
99ABFC-159A	37.887234	107.669373	Upper Cement	Iron spring	dry	5	T	6 to .5	Large iron spring deposit, finely laminated hydrous iron oxides with plant material, twigs appear very young, sample from talus slope on south side of South Fork Cement Creek above confluence.	*5YR-4/6* yellowish red
99ABFC-164A	37.870098	107.655220	Upper Cement	Iron spring	spring	2	colluvium	10 to 0	Colluvial ferricrete, fine-grained matrix sampled, probably an iron spring deposit, head of South Fork Cement Creek.	*5YR-4/6* yellowish red
99VMS-37	37.849445	107.727798	Middle Cement	Iron spring	spring	1	-	-	Brown, organic-rich iron spring deposit, saddle along ridge between Mineral and Cement Creeks, south of Ohio Peak.	no data
99VMS-65A	37.865276	107.725830	Mineral Cr	Iron spring	dry	2	-	-	Brown iron from outcrop of paleo spring just south of Chattanooga beaver ponds.	no data
99VMS-65B	37.865276	107.725830	Mineral Cr	Iron spring	dry	1	-	-	Light-brown iron from outcrop of paleo spring just south of Chattanooga beaver ponds.	no data
ODY98-32a	37.833076	107.609062	Mineral Cr	Iron spring	spring	2	-	-	Top of 8-in. long core in active iron spring consists of angular pebble-size clasts in a medium-brown sand-size matrix (north-draining tributary to Middle Fork Mineral Creek).	*5YR-3/4* dk reddish brown
ODY98-32c	37.833076	107.646027	Mineral Cr	Iron spring	spring	1	-	-	Bottom of 8-in. long core in active iron spring consists of fine silt to sand-size sediment, dark brown in hand sample (north-draining tributary to Middle Fork Mineral Creek).	*2.5YR-3/6* dk red
00ABFC-230	37.919400	107.664452	Cal Gulch	manganocrete	Mn	5	-	-	Alluvial deposit, small rounded gravel clasts with manganese-oxide rich matrix (sampled in California Gulch).	no data
00CGS-1150	37.923161	107.650688	Cal Gulch	manganocrete	Mn	5	-	-	Black matrix of subangular clasts conglomerate.	no data
99VAS-01	37.919548	107.637695	Cal Gulch	manganocrete	Mn	5	-	-	Upper California Gulch, black precipitate as apron at spring, matrix supported.	no data
99VMS-13A1	37.868332	107.646286	Mineral Cr	manganocrete	Mn	5	-	-	Black matrix from outcrop of draining adit above Chattanooga beaver ponds, Ferricrete mine.	no data
HPDY00-13	37.910595	107.710800	Cal Gulch	manganocrete	Mn	5	-	-	Colluvial manganocrete deposit consists of subangular cobbles and pebbles, some boulder-size clasts in a granular, managanese and iron-cemented matrix (in Placer Gulch below Gold Prince mine).	*7.5YR-2.5/2* very dk brown

Field No.	Latitude N. (degrees)	Longitude W. (degrees)	Reach	Deposit type	Wet/Dry	Dominant iron mineral[1]	Geomorphologic unit[2] (Vincent and others, this volume)	Age range of host deposit (per 1,000 years)	Site description	Munsell Color code (Goddard and others, 1948)
HPDY00-16	37.904644	107.730995	Animas	manganocrete	Mn	5	-	-	Alluvial manganocrete deposit consists of subround to subangular pebble-size clasts, in a sand-size, manganese-rich cemented matrix (base of alluvial fan in Eureka Gulch).	*7.5YR-3/3* dk brown
HPDY00-4	37.923977	107.701668	Cal Gulch	manganocrete	Mn	5	-	-	Alluvial manganocrete deposit consists of subangular pebble- to cobble-size clasts in a sand-size manganese-rich cemented matrix (base of alluvial fan in California Gulch).	*10YR-4/3* brown
HPDY00-6	37.906002	107.726669	Animas	manganocrete	Mn	5	-	-	Colluvial manganocrete deposit consists of angular to subangular pebble- and cobble-size clasts in a granular, sand-size manganese and iron-cemented matrix (at head of Eureka Gulch).	*7.5YR-2.5/3* very dk brown
00ABM-275	37.844223	107.676445	Mineral Cr	mine-impacted	mine	1	mine ppt	0	Bonner mine precipitate.	*2.5YR-3/6* dk red
99VMS-10	37.851429	107.644257	Mineral Cr	mine-impacted	spring	5	mine ppt	0	Iron floc from seep in colluvium 30 ft upstream of Burro Bridge, east side of Mineral Creek; possibly from caved adit(?).	no data
99VMS-13A2	37.868332	107.647652	Mineral Cr	mine-impacted	dry	5	mine ppt	0	Brown matrix from outcrop of draining adit above Chattanooga beaver ponds, Ferricrete mine.	*5Y-3/4* dk reddish brown
99VMS-13B	37.868332	107.679100	Mineral Cr	mine-impacted	mine	1	mine ppt	0	Brown floc from effluent of adit above Chattanooga beaver ponds, Ferricrete mine.	*2.5YR-4/8* red
99ABFC-102Ar	37.889351	107.668333	Upper Cement	rep	exclude	1	T	6 to .5	Replicate sample.	*5YR-3/4* dk reddish brown
99ABFC-122D2	37.880260	107.665688	Upper Cement	rep	exclude	2	T	4 to .5	Replicate sample (wet sample preserved for mineralogical analysis).	no data

[1]Mineralogy: 1=schwertmannite; 2=goethite; 3=jarosite; 4=pyrite; 5=amorphous iron oxides.

[2]p = flood plain, T = terrace; bed =streambed; Fo = old fan; Fy = young fan; Tg = gravel terrace; "-" = not determined.

Table 3. Characteristics of ferricrete sampled in this study.

Type of ferricrete	No. of samples	Typical iron-oxide mineralogy	Typical sedimentary features	Depositional environment	Observed range in water pH	Major-element chemistry
Precipitate-type		**(commonly wet)**				
Bog iron	26	Schwertmannite>	Few clasts;	Shallow wetlands		<2 wt. % Al
Iron spring	15	goethite>	sometimes banded.	Sides of valleys		40–60 wt. % Fe
Total	41	ferrihydrite			3.0 to 4.5	1–3.5 wt. % S
Conglomerate-type		**(commonly dry)**				
Alluvial	21	Goethite>	Rounded clasts or	Stream terraces		3–5 wt. % Al
Colluvial	16	schwertmannite>	subangular clasts.	Hillslope deposits		25–35 wt. % Fe
Total	37	ferrihydrite			3.0 to 6.6	<1.25 wt. % S
Manganocrete		**(wet or dry)**				
(predominantly the colluvial-type was sampled)	8	Manganese-rich ferrihydrite.	Rounded clasts or subangular clasts.	Colluvial or alluvial deposits.	4.5 to 4.8	6–9 wt. % Al <8 wt. % Fe <0.5 wt. % S

Sampling bias must be considered because ground water could not be collected at depth. Samples were only collected where seeps and springs emerge at the ground surface. Small differences in sampling approach by different coauthors also could contribute to bias. In Cement Creek, the precise sampling location was selected on the basis of low dissolved-oxygen content, whereas in Mineral Creek, dissolved oxygen was not measured and other field criteria, such as pH and conductivity, were used to select the sampling site. Water samples collected for this study represent a variety of non-equilibrium surficial conditions, and thus may not collectively represent the pH and mineral solubilities of deeper circulating ground water. While recognizing the potential for bias, we attribute the large spatial differences in ground-water chemistry primarily to differences in pH that correlate spatially with the degree of iron-sulfide mineralization and the irregular distribution of saturated fractures.

The geochemical modeling program PHREEQCI (version 2.7.1, Parkhurst and Appelo, 1999) was used to determine speciation and state of saturation with respect to secondary mineral phases for the water samples in table 1. A log activity of –18.0 for schwertmannite as determined by Bigham, Schwertmann, and others (1996), was added to the WATEQ4F thermodynamic database (Ball and Nordstrom, 1991) used with PHREEQE. Iron solubility was calculated for common iron solid-phase species including amorphous ferrihydrite [$Fe(OH)_3$ (a)], goethite (FeOOH), potassium or K-jarosite ($KFe_3(SO_4)_2(OH)_6$), and schwertmannite ($Fe_8O_8(OH)_{4.5}(SO_4)_{1.75}$). In Mineral Creek, $Fe(OH)^{+2}$ was the most abundant dissolved species of Fe^{+3} for all but one sample, whereas in upper Cement Creek, $FeSO_4^-$ was the dominant dissolved-iron species for 9 out of 12 samples. For the most part, $FeSO_4^-$ was the dominant aqueous iron species whenever pH <4.0, which was more common in Cement Creek. Spatial differences in iron speciation and pH are dynamic, and variability may be attributed in part to the rock chemistry, length of the flow path, degree of mixing, and to diurnal and seasonal variations in hydrologic conditions.

Plots of pH versus the log activity of iron (pFe) are a conventional way of representing the solubility of minerals, assuming log activity of sulfate (pSO_4) is constant. Figure 2 is a plot of pFe versus pH for the minerals ferrihydrite, goethite, potassium jarosite, and schwertmannite. Mineral species most likely to precipitate have positive or near-zero log activities, and thus plot in the positive or lower half of the graph. Data in figure 2 and table 4 indicate that all of the sampled iron-rich ground water is saturated with goethite, more than half of the water is saturated with schwertmannite and potassium jarosite, and slightly less than half the samples are saturated with ferrihydrite ($Fe(OH)_3$). Bigham, Schwertmann, and others (1996) and Yu and others (1999) have shown that schwertmannite solubility is intermediate between the solubilities of potassium jarosite and goethite. Many of these water samples are not fully equilibrated with oxygen, which may account for some of the undersaturated values. Complete saturation with oxygen would tend to further increase saturation (precipitation) of iron hydroxide minerals, and decrease the remaining iron in solution. The data show that iron saturation is common and occurs in a wide range of pH values. Iron saturation occurs in both mining-impacted and non-impacted ground water discharging to acidic springs throughout the Cement Creek and Mineral Creek watersheds.

In addition to the iron hydroxide minerals shown in figure 2, iron-rich ground water was highly saturated or near saturation with respect to amorphous SiO_2 (crystobalite; table 4), sulfate minerals including gypsum ($CaSO_4 \cdot 2H_2O$), anhydrite ($CaSO_4$), celestite ($SrSO_4$), melanterite ($FeSO_4 \cdot 7H_2O$); and with hydroxide minerals alunite ($KAl_3(SO_4)_2(OH)_6$), gibbsite ($Al(OH)_3$), and amorphous $Al(OH)_3$. In contrast, manganese-rich ground water was undersaturated

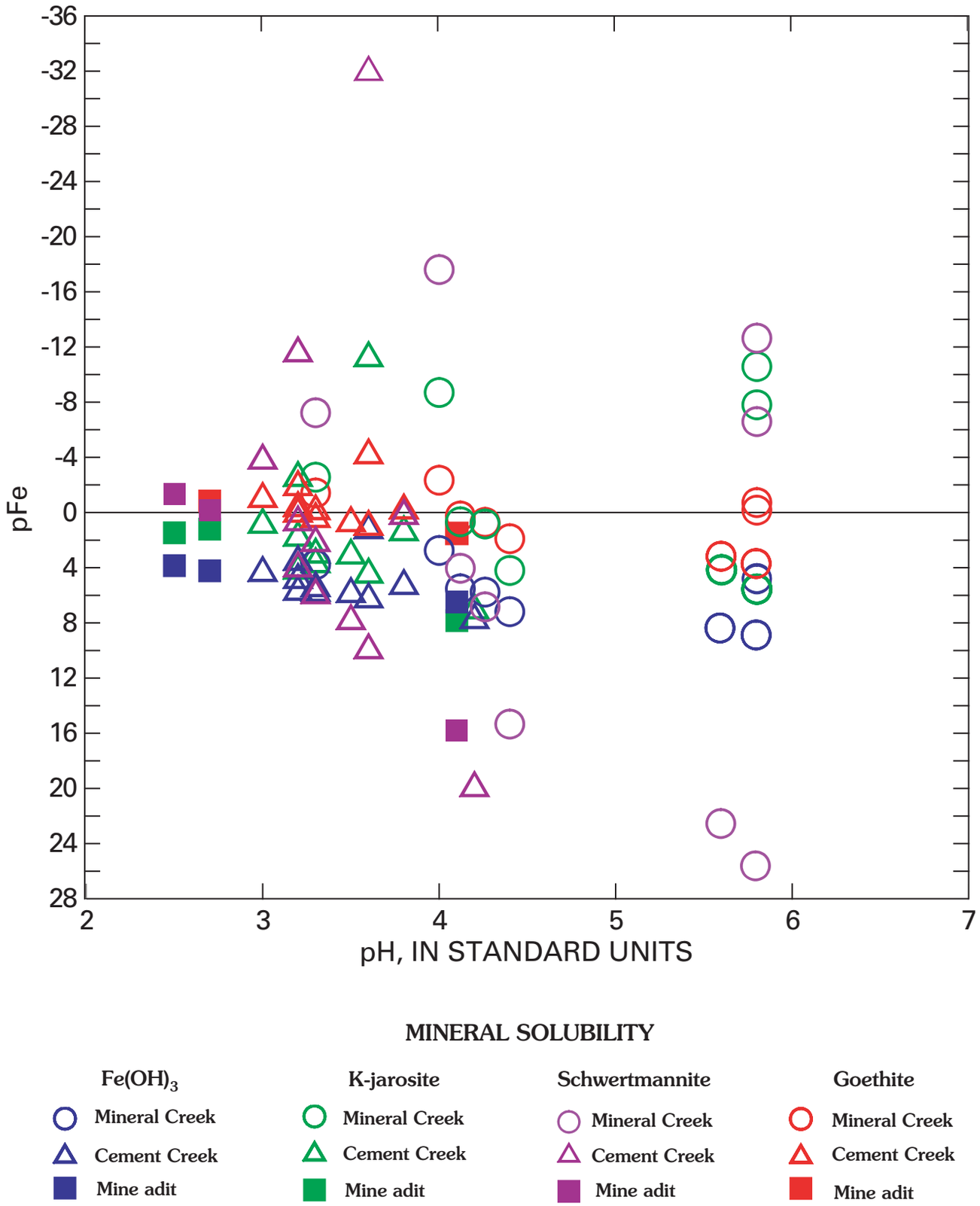

Figure 2. Plot of log activity of iron (pFe) versus pH for iron-rich ground water in Animas River watershed study area. A positive pFe value indicates that the mineral is likely to precipitate from solution.

Table 4. Saturation indices (log activities) for iron oxyhydroxide minerals and crystobalite in iron-rich ground water in Cement and Mineral Creeks.

[See figures 1 and 2. Activity data calculated in PHREEQCI 2.7.1 using modified WATEQ4F database with log activity of –18.0 for schwertmannite, based on Bigham, Schwertmann, and others (1996). A positive saturation indices value (italic) indicates that the solution is saturated with respect to that mineral]

Site	Date	Reach	pH	pe[1]	Eh[1]	Fe(II) (µg/L)	Fe(III) (µg/L)	Saturation indices: Ferrihydrite $Fe(OH)_3(a)$[2]	Goethite FeOOH	K-jarosite $KFe_3(SO_4)_2(OH)_6$	Schwertmannite $Fe_8O_8(OH)_{4.5}(SO_4)_{1.75}$	Crystobalite $SiO_2(a)$
Iron-bearing springs:												
99VMF10*	8/15/1999	Mineral Creek	6.57	6.98	0.388	6.9	6.9	*4.16*	*9.35*	*5.16*	*26.79*	*0.26*
99VMF34	8/24/1999	Mineral Creek	5.81	5.15	0.294	0.05	<0.05	–0.72	*4.76*	–10.58	–12.64	–0.36
99VMF67	8/24/1999	Mineral Creek	4.16	8.76	0.479	<0.01	<0.01	–0.17	*4.84*	–7.81	–6.59	*0.27*
99VMF68	8/24/1999	Mineral Creek	3.99	11.95	0.657	<0.01	<0.01	–2.34	*2.75*	–8.70	–17.61	*0.28*
99VMF92	9/1/1999	Mineral Creek	4.41	10.98	0.614	8.4	8.0	*1.90*	*7.19*	*4.20*	*15.34*	*0.24*
99VMF72	8/25/1999	Mineral Creek	3.33	11.87	0.659	1.2	0.3	–1.42	*3.77*	–2.57	*11.89*	*0.24*
00VMF01	9/6/2000	Mineral Creek	4.26	9.85	0.541	30	0.54	*0.70*	*5.77*	*0.83*	*6.84*	*0.53*
00VMF03	8/31/2000	Mineral Creek	4.12	10.60	0.593	4.2	0.49	*0.25*	*5.53*	*0.66*	*4.04*	*0.13*
PG fan	8/19/2002	Cement Creek	3.32	11.89	0.670	38	18.1	*0.15*	*5.52*	*3.42*	*5.69*	*0.42*
YS-LB	10/25/2000	Cement Creek	3.51	12.03	0.665	20	11	*0.46*	*5.60*	*2.80*	*7.56*	*0.00*
YS-RB	10/25/2000	Cement Creek	3.22	11.89	0.661	20	9	–0.64	*4.58*	*1.49*	*0.40*	*0.15*
Gas Spring	8/23/2002	Cement Creek	4.15	11.59	0.644	26	34	*2.28*	*7.49*	*6.78*	*19.67*	*0.48*
Ren Spg	8/23/2002	Cement Creek	3.55	12.19	0.680	13	16	*0.73*	*5.97*	*4.18*	*9.67*	*0.40*
UB-1	10/25/2000	Cement Creek	3.15	12.04	0.697	20	45	–0.22	*5.43*	*3.89*	*3.74*	–0.02
GT-1	9/24/1999	Cement Creek	3.20	12.35	0.699	0.15	0.29	–2.16	*3.26*	–2.84	–11.85	*0.35*
GT-2	9/27/1999	Cement Creek	3.00	11.85	0.668	17	9.3	–1.30	*4.06*	*0.56*	–4.07	*0.31*
GT-3	9/27/1999	Cement Creek	4.62	4.88	0.277	43	0	–3.00	*2.45*	–9.11	–23.30	*0.28*
GT-4	9/27/1999	Cement Creek	3.79	9.65	0.549	67	0.7	–0.46	*5.04*	*1.11*	–0.06	*0.29*
GT-7	9/27/1999	Cement Creek	3.33	11.56	0.664	23	12	–0.41	*5.16*	*2.72*	*1.90*	*0.21*
GT-8	9/27/1999	Cement Creek	3.59	8.40	0.477	0.32	0.004	–4.47	*0.96*	–11.51	–32.22	*0.16*
Mining-affected springs or adit of inactive mine:												
L3A (adit)	9/29/1999	Prospect Gulch	4.14	10.09	0.549	22	0.4	*1.50*	*6.47*	*7.82*	*15.80*	*1.86*
JJP (adit)	9/29/1999	Prospect Gulch	2.73	14.86	0.815	0.41	62	–0.84	*4.21*	*1.19*	–0.15	*0.56*
H7A (adit)	9/29/1999	Prospect Gulch	2.52	13.55	0.740	23	268	–1.17	*3.84*	*1.43*	–1.36	–0.03
99VMF13	8/23/1999	Mineral Creek	5.75	8.62	0.476	12	12	*3.72*	*8.86*	*5.51*	*25.55*	*0.25*
99VMF12	8/23/1999	Mineral Creek	5.62	9.07	0.500	5.8	5.8	*3.28*	*8.38*	*4.25*	*22.49*	*0.25*

[1]Calculated on the basis of relative concentrations of iron species (Fe^{+2}/Fe^{+3}).

[2](a) = amorphous.

*Possibly mining affected (table 1).

with respect to alunite and gibbsite, although saturated with respect to amorphous $Al(OH)_3$ and amorphous SiO_2. Water samples from California Gulch were highly saturated with respect to manganese-bearing minerals including manganite (MnOOH), rhodochrosite ($MnCO_3$), and pyrolusite (MnO_2) as well as with carbonate minerals, commonly calcite and aragonite ($CaCO_3$), and dolomite ($CaMg(CO_3)_2$). The occurrence of manganese-rich ground water is consistent with dissolution of pyroxmangite ($(Mn,Fe,Ca,Mg)SiO_3$) and rhodochrosite from ore veins throughout the Eureka Gulch area.

Figure 3 is a plot of pe versus pH and a phase diagram for the Fe-S-K-O-H system calculated using the solubility product ($K_{sp} = -18.0$) for schwertmannite, as determined by Bigham, Schwertmann, and others (1996). Potential energy (pe—referring to the redox states of ion pairs) as a function of Eh was calculated in PHREEQCI, on the basis of total Fe^{+2} and Fe^{+3} concentrations. Over the pH range of 3 and 4.5, schwertmannite is the dominant phase for most of the iron-rich ground water in Cement Creek and Mineral Creek. For the two mine adit samples with pH <3, jarosite is metastable with respect to schwertmannite and goethite. Above a pH of 5, ferrihydrite is the dominant form, but it too has an overlapping stability field with schwertmannite at lower pH and goethite at lower pe. Only two Mineral Creek samples plot in the overlapping schwertmannite-goethite stability field and one Mineral Creek sample (pH=5.8) was in the schwertmannite-ferrihydrite transitional field. Based on other studies (Bigham, Schwertmann, and others, 1996; Bigham, Schwertmann, and Pfab, 1996; Yu and others, 1999), goethite either precipitates directly or forms by hydrolysis from schwertmannite or ferrihydrite. Samples from this study plot predominantly in the non-overlapping part of the schwertmannite field. This is consistent with mineralogical analyses presented in the next section, showing both schwertmannite and goethite as the most common iron oxyhydroxide minerals in Mineral and Cement Creek basins.

Solid-Phase Geochemistry of Iron-Cemented Deposits and Stream Sediment

The major-element and trace-element chemistry of the solid-phase samples (table 2) is evaluated with respect to deposit type, mineralogy, relative age of the host deposit, spatial location, and whether the deposit appeared to be actively precipitating iron.

Deposit Type

Alluvial and colluvial ferricrete, bog iron, iron spring, and manganocrete deposits were sampled to identify major chemical characteristics for each deposit type. As a point of reference, the solid-phase chemistry of iron and manganese cemented deposits is compared with that of premining and modern stream sediment collected by Church, Fey, and Unruh (this volume).

The distribution of major and trace elements among the solid-phase ferricrete and stream-deposited sediment varied substantially. The range in selected major elements (Al, Ca, Fe, K, Mg, and S) and trace elements (As, Cd, Cu, Mn, Pb, and Zn) is depicted by a series of box plots (fig. 4) that are grouped by ferricrete deposit type. The most obvious difference between the deposit types among the major elements is the iron content (fig. 4). Bog iron, iron spring, and mining-affected precipitates had nearly twice as much iron by weight percent as did alluvial and colluvial ferricrete. The iron content by weight in the matrix of most alluvial and colluvial ferricrete samples was between about 25 and 35 percent. Assuming that most of the iron cement is present as FeOOH (goethite), this accounts for about 40–55 percent of the total weight of the digested matrix. In contrast, the iron content of most bog iron and spring deposits is considerably higher, ranging from about 40 to 60 percent Fe—or 63 to as much as 95 percent goethite, by weight. If one alternately assumes that a major fraction of the iron is amorphous schwertmannite ($Fe_8O_8(OH)_{4.5}(SO_4)_{1.75}$), the weight fraction in some of the samples can exceed 100 percent, consistent with X-ray diffraction results indicating that more than one form of iron oxide is present.

We attribute the greater weight percentages of aluminum, calcium, potassium, and magnesium in the alluvial and colluvial ferricrete samples (fig. 4) to a bias introduced by the sample-preparation method. Whereas the bog iron and spring samples consist of relatively pure iron-oxide precipitate, it was virtually impossible to completely disaggregate the chemically precipitated matrix from sand and silt derived from the depositional environment. Thus, the matrix of alluvial and colluvial ferricrete samples tended to have a greater weight percent of common rock-forming minerals than did the mining-affected precipitates, bog iron, and iron spring samples.

Of the major elements reported by ICP-MS, aluminum had the highest concentration, with the exception of iron. Alluvial and colluvial ferricrete had between 3 and 5 percent aluminum by weight, and bog iron and spring deposits generally had considerably less than 2 percent by weight. Manganocrete samples had the highest aluminum concentrations, generally between 6 and 9 percent. In contrast with the iron-rich samples, manganocrete contained less than 5 percent iron by weight but had the most magnesium, aluminum, and potassium of all the deposit types, with the exception of premining and modern stream sediment. Manganocrete samples also had the largest concentrations of cadmium, copper, lead, zinc—and (of course) manganese. Iron springs and bogs generally had between 1.0 and 3.5 weight percent sulfur, compared with <1.25 percent for colluvial-type ferricrete and manganocrete samples. The larger sulfur content corresponds with greater acidity and a predominance of schwertmannite as the dominant iron mineral in bog iron and spring samples. Bog iron and spring deposits have the largest individual occurrences of arsenic and are generally lower in copper, lead, and manganese.

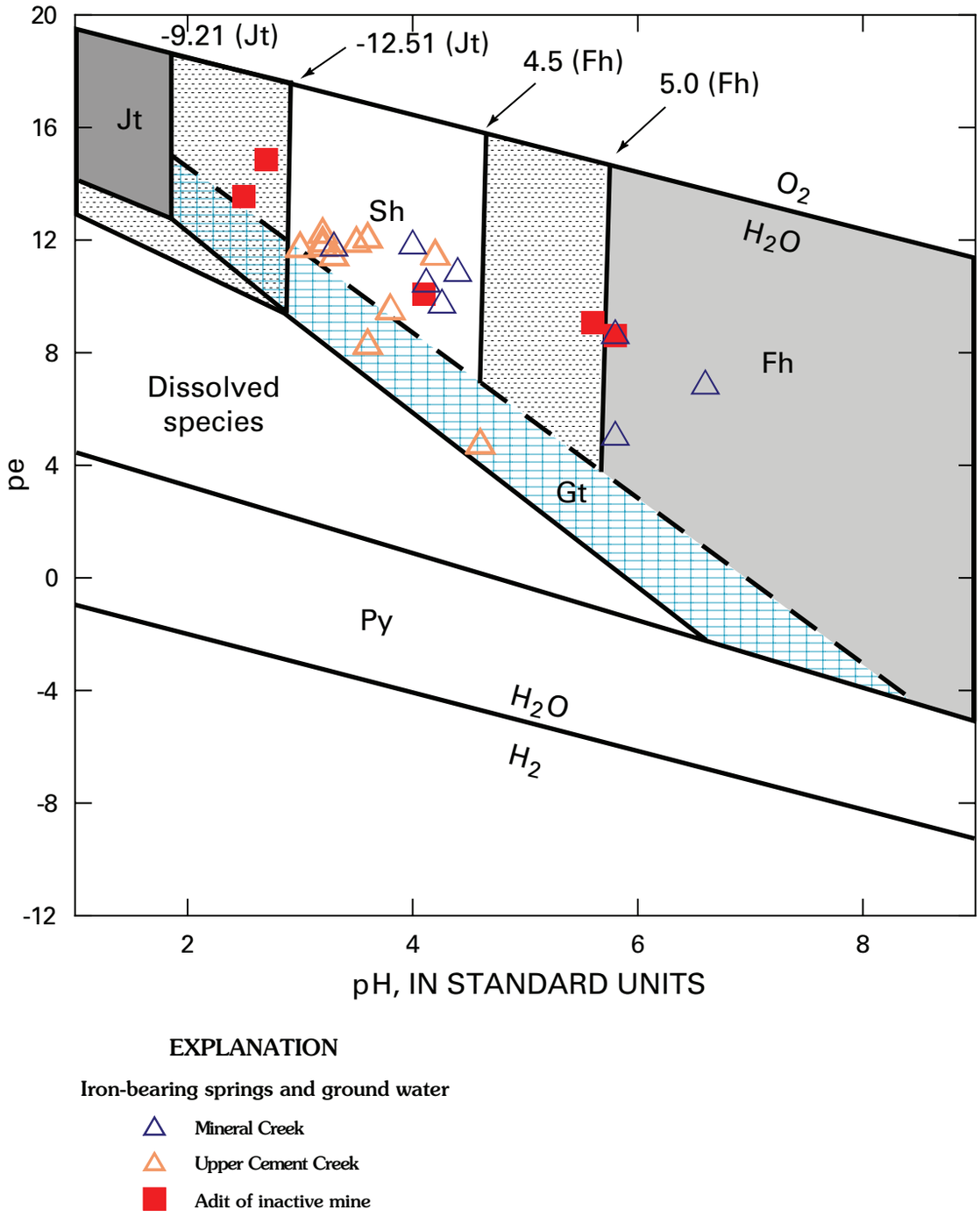

Figure 3. Phase diagram for Fe-S-K-O-H system showing pe versus pH at 25°C (modified from Bigham, Schwertmann, and others, 1996), and iron-rich ground-water samples from Animas River watershed study area. Log activity defined as pe=Eh/59.2; total log activities of Fe^{+2}=–3.47; Fe^{3+}=–3.36 or –2.27; SO_4^{2-}=–2.32; K^+=–3.78. Solid-phase iron minerals include Jt, K-jarosite; Sh, schwertmannite; Fh, ferrihydrite; Gt, goethite; Py, pyrite. Line equations are Gt(pe=17.9–3pH); Jt(pe=16.21–2pH); Fh(pe=21.50–3pH); Sh(pe=19.22–2.6 pH), and Py (pe=5.39–1.14pH). Field of goethite metastability shown by dashed line. Dot pattern demonstrates expansion of K-jarosite and ferrihydrite fields if lower log K's are selected.

The distribution of major elements was consistent with the composition of major rock-forming minerals identified by X-ray diffraction. Stream-deposited sediment represented a composite of the major rock-forming minerals in the study area. Quartz was by far the most abundant rock-forming mineral in the cement from alluvial and colluvial ferricrete samples, followed by albite and muscovite. Trace levels of clinochlore, rutile, orthoclase, and montmorillonite were also present in some samples. The same minerals were also found in bog iron and spring deposits, albeit in lesser amounts, and probably represent fine-grained fluvial or windblown particles trapped by the bogs and springs. Likewise, minerals identified in the manganocrete and in the over-bank sediment samples primarily included quartz, followed by albite and muscovite, with few other trace minerals. Gangue and ore-bearing veins in the Sunnyside mine described by Casadevall and Ohmoto (1977) commonly included quartz (30–35 percent), sphalerite (10–15 percent), galena (10–15 percent), pyroxmangite ($MnSiO_3$) (10–15 percent), pyrite (6–8 percent), rhodochrosite (5–8 percent), chalcopyrite (3–5 percent), tetrahedrite (1–4 percent), calcite (1 percent), fluorite (1 percent); plus a variety of minerals with typically less than 0.5 percent abundance, including hematite, gold, anhydrite, sericite, bornite, barite, and gypsum.

In comparison to iron springs and bogs, conglomerate-type ferricrete had similar ranges in mean concentration for cadmium and zinc, but this sample group tended to be lower in sulfur and elevated in concentrations of copper, manganese, and lead. Generally, acidic pH favors the adsorption of anion species such as arsenic and sulfate, whereas near-neutral pH favors the adsorption of cations such as copper, manganese, and lead (Dzombak and Morel, 1987, 1990). Cadmium and zinc are common in ore minerals and thus common in water affected by mine drainage, but concentrations of these two trace elements did not vary substantially among ferricrete deposit types, despite probable differences in pH environment.

Mineralogy

Iron mineralogy varied substantially among the deposit types (fig. 5). For the alluvial and colluvial ferricrete samples, the most abundant iron mineral is goethite, although commonly in combination with schwertmannite. For two-thirds of the bog iron and iron spring samples, the major iron mineral identified was schwertmannite, usually with secondary goethite. The dominant iron mineral for the remaining third of bog iron and spring samples was goethite.

Fifteen of the eighty-six solid-phase samples were not included in figure 5 because they did not form statistically viable sample groups ($n \leq 5$) or had possible mining influences (as indicated by Mast and others, this volume). Amorphous iron oxide was the only iron mineral identified in the five manganocrete samples, which also were not included in figure 5. Two iron spring samples and five alluvial and colluvial ferricrete samples had ferrihydrite as the dominant mineral. Also not included were two samples of wet alluvial ferricrete from the Gladstone to Fairview reach of Cement Creek, which had schwertmannite as the dominant iron mineral.

As mentioned in the previous section, sulfur in schwertmannite's mineral lattice accounted for greater concentrations of sulfur in the bog iron and iron spring deposit types. Schwertmannite is a poorly crystalline, yellowish-brown mineral formed by the oxidation of Fe (II) in acid-sulfate systems (Bigham and others, 1990; Bigham and others, 1994; Bigham, Schwertmann, and others, 1996; Bigham, Schwertmann, and Pfab, 1996). It has a high specific-surface area, usually in the range of 100–200 m^2/g; with a fibrous or "pin-cushion" morphology (Bigham, Schwertmann, and Pfab, 1996). Bigham, Schwertmann, and Pfab (1996) observed the gradual transformation of schwertmannite by hydrolysis to goethite in the laboratory over a period of 543 days via the overall reaction:

$$Fe_8O_8(OH)_{4.5}(SO_4)_{1.75(s)} + 2.5H_2O_{(l)} \rightarrow 8FeOOH_{(s)} + 2.5H^+_{(aq)} + 1.25SO_4^{2-}{}_{(aq)} \quad (5)$$

Yu and others (1999) have shown that metastability for schwertmannite is significantly affected by water temperature and by variations in the activity of dissolved sulfate.

At several localities we have identified banded specimens of schwertmannite with goethite and (or) ferrihydrite or jarosite. At least three sites had alternate banding of thin layers of yellow schwertmannite and dark-brown goethite. The banding is presumably caused by seasonal differences in environmental conditions such as pH and Eh conditions, the degree of seasonal variability at the time of precipitation such as wetting and drying, and (or) subsequent degree of surficial exposure and aging.

Iron spring and bog iron deposits dominated by schwertmannite had similar levels of trace-element concentrations as the iron spring and bog iron deposits dominated by goethite, which suggests that the aging transformation to goethite does not produce a net release of trace elements to the environment. Trace elements may sorb to the mineral surfaces or be present as a solid-series phase within the crystalline lattice. Either process could allow for relatively high concentrations of trace elements in the iron-oxide cements.

Age of Iron Minerals

Understanding the age of iron cementation is important for two reasons. First, some amorphous or poorly crystalline minerals are thought to undergo a transformation to a relatively more structured crystalline lattice with time—schwertmannite or jarosite to goethite, for example. Second, speciation of iron oxyhydroxide minerals such as schwertmannite and jarosite is pH sensitive, and thus the type of iron mineral may indicate pH and Eh conditions during the time the mineral formed. Such information helps to establish the pH of geochemical baselines prior to mining.

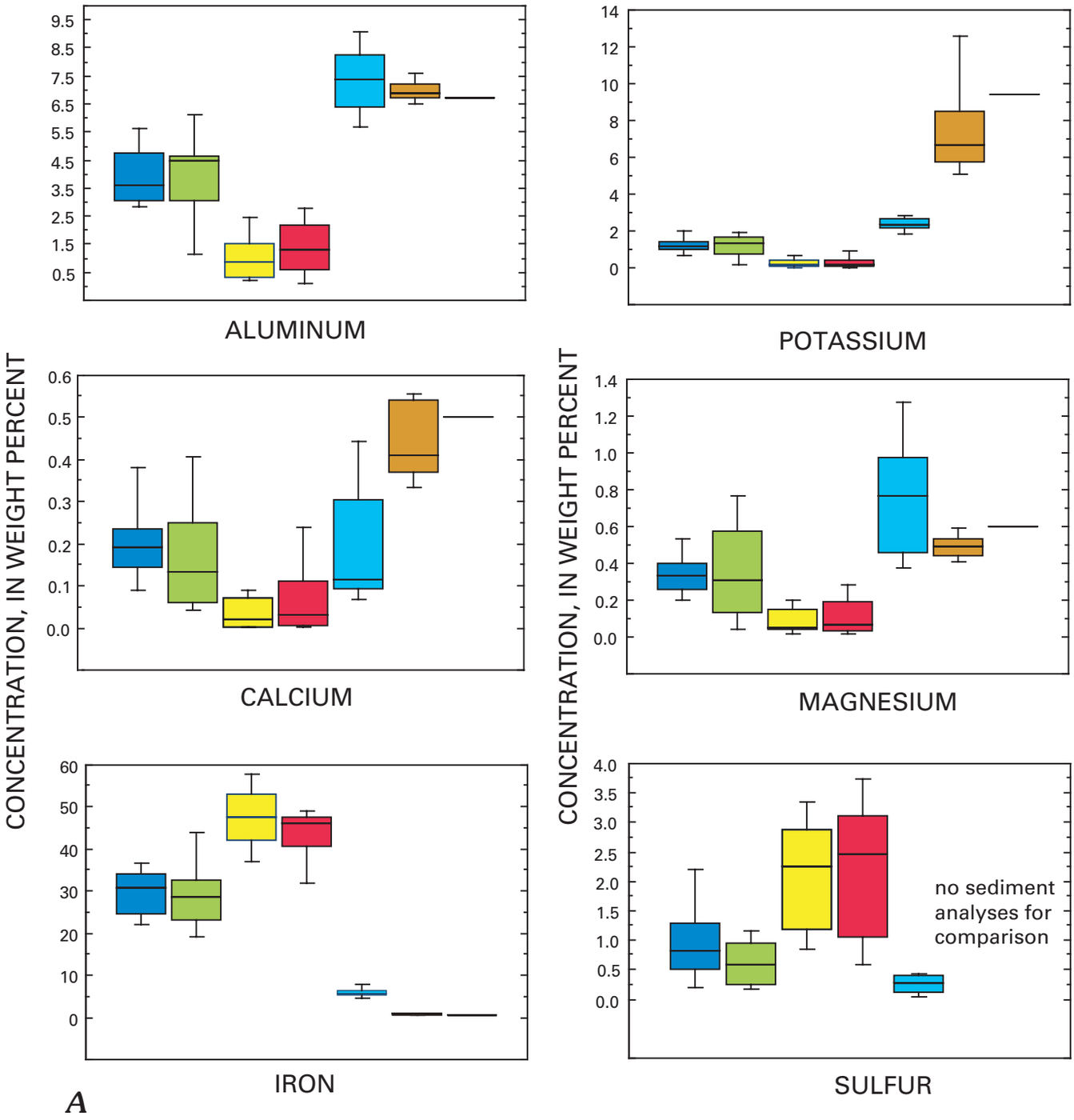
ALUMINUM
POTASSIUM
CALCIUM
MAGNESIUM
IRON
SULFUR
CONCENTRATION, IN WEIGHT PERCENT
CONCENTRATION, IN WEIGHT PERCENT
no sediment analyses for comparison
A
EXPLANATION
Alluvial ferricrete (21)
Colluvial ferricrete (16)
Iron bog (26)
Iron spring (15)
Manganocrete (8)
Premining sediment (39)
Modern sediment (10)
The information displayed in box plots is summarized in the graphic below.
90th percentile
75th percentile
Median
25th percentile
10th percentile

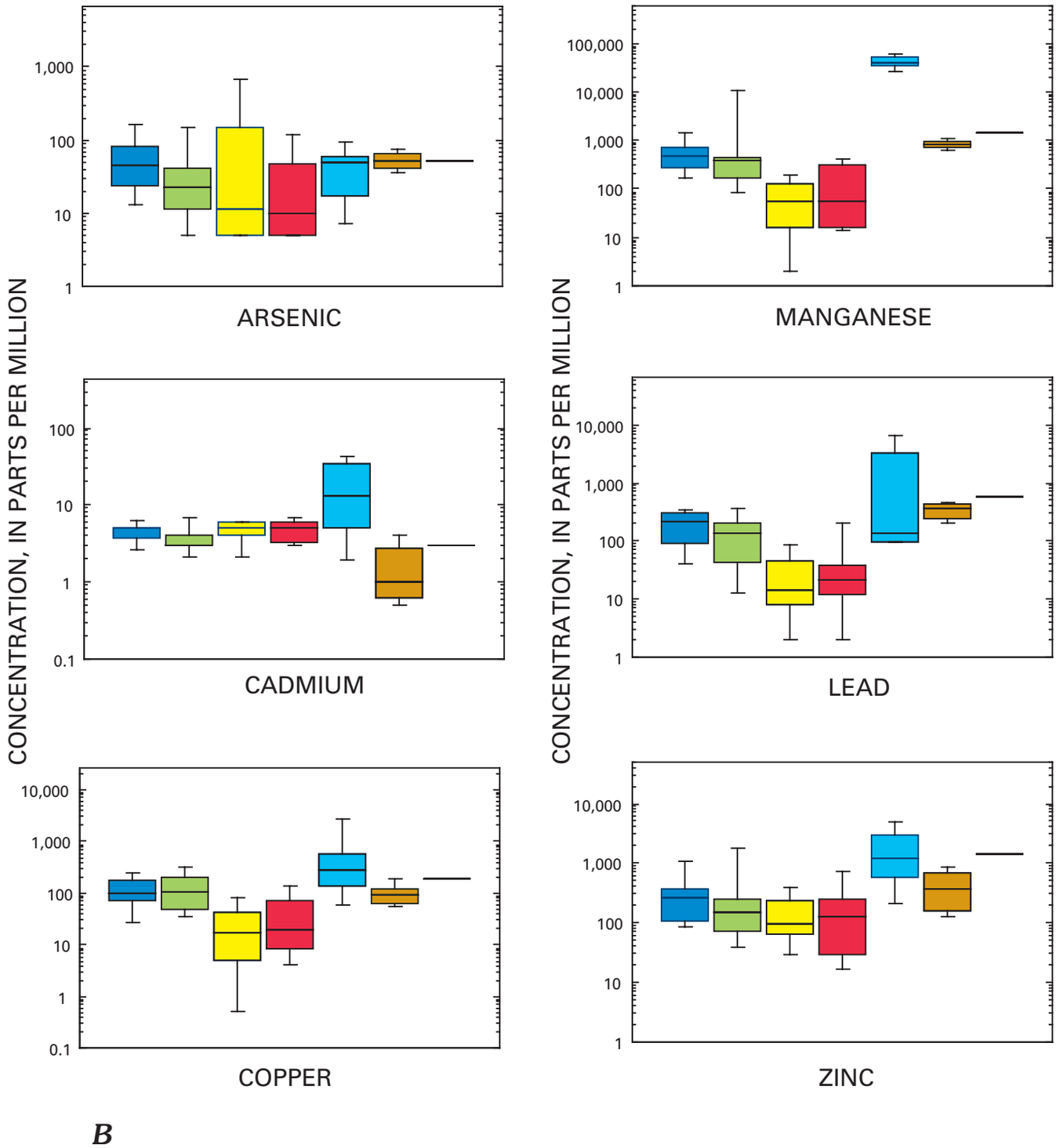

Figure 4 (above and facing page). Box plots showing selected solid-phase elements grouped by ferricrete deposit type. *A*, major elements in weight percent; *B*, trace elements in parts per million. Order of box plots is same as sequence in explanation.

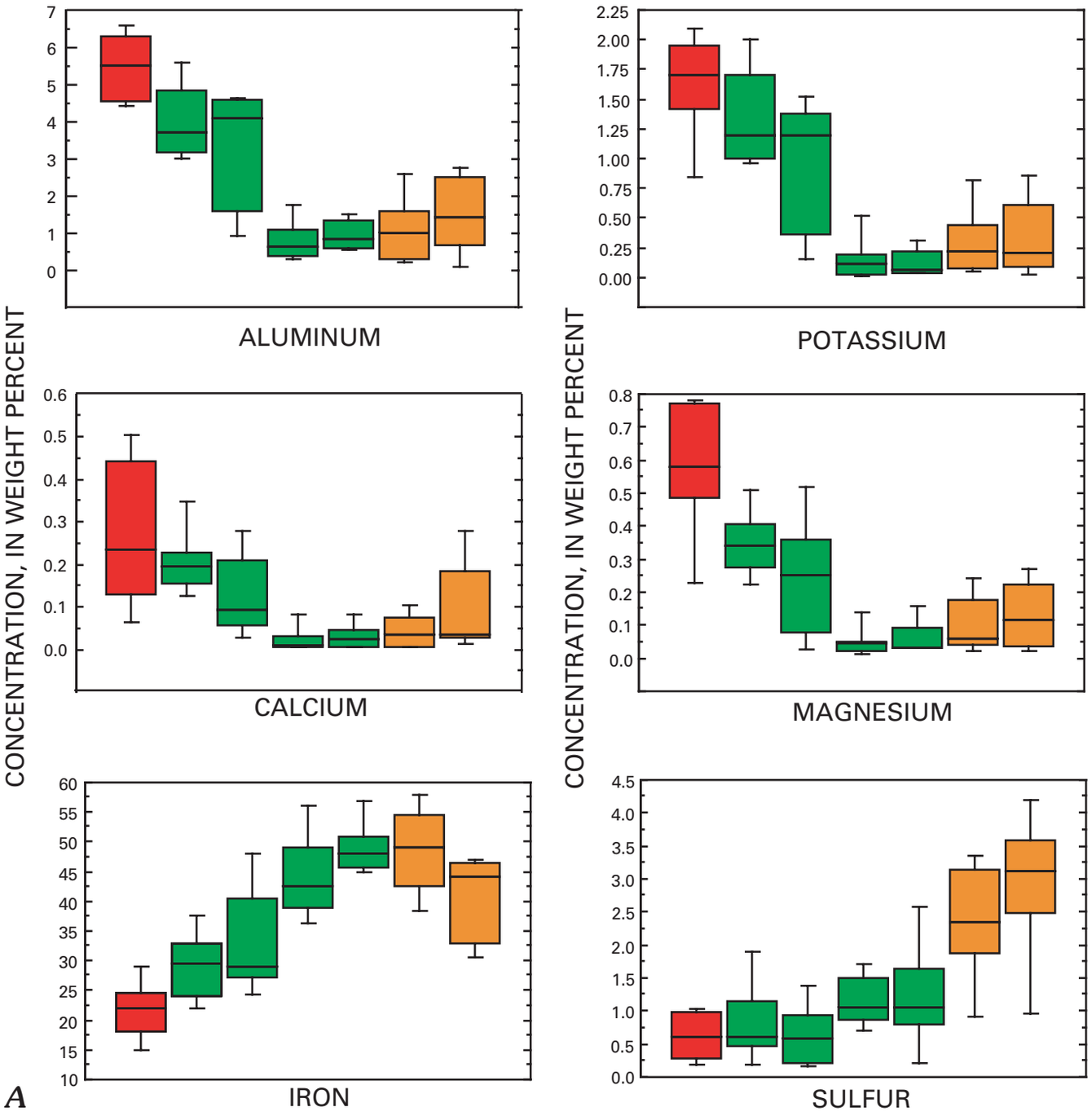
ALUMINUM
POTASSIUM
CALCIUM
MAGNESIUM
IRON
SULFUR
CONCENTRATION, IN WEIGHT PERCENT
CONCENTRATION, IN WEIGHT PERCENT
A
EXPLANATION
Ferrihydrite
Colluvial ferricrete (5)
Goethite
Alluvial ferricrete (16)
Colluvial ferricrete (11)
Iron bogs (6)
Iron springs (5)
Schwertmannite
Iron bogs (20)
Iron springs (8)
The information displayed in box plots is summarized in the graphic below.
90th percentile
75th percentile
Median
25th percentile
10th percentile

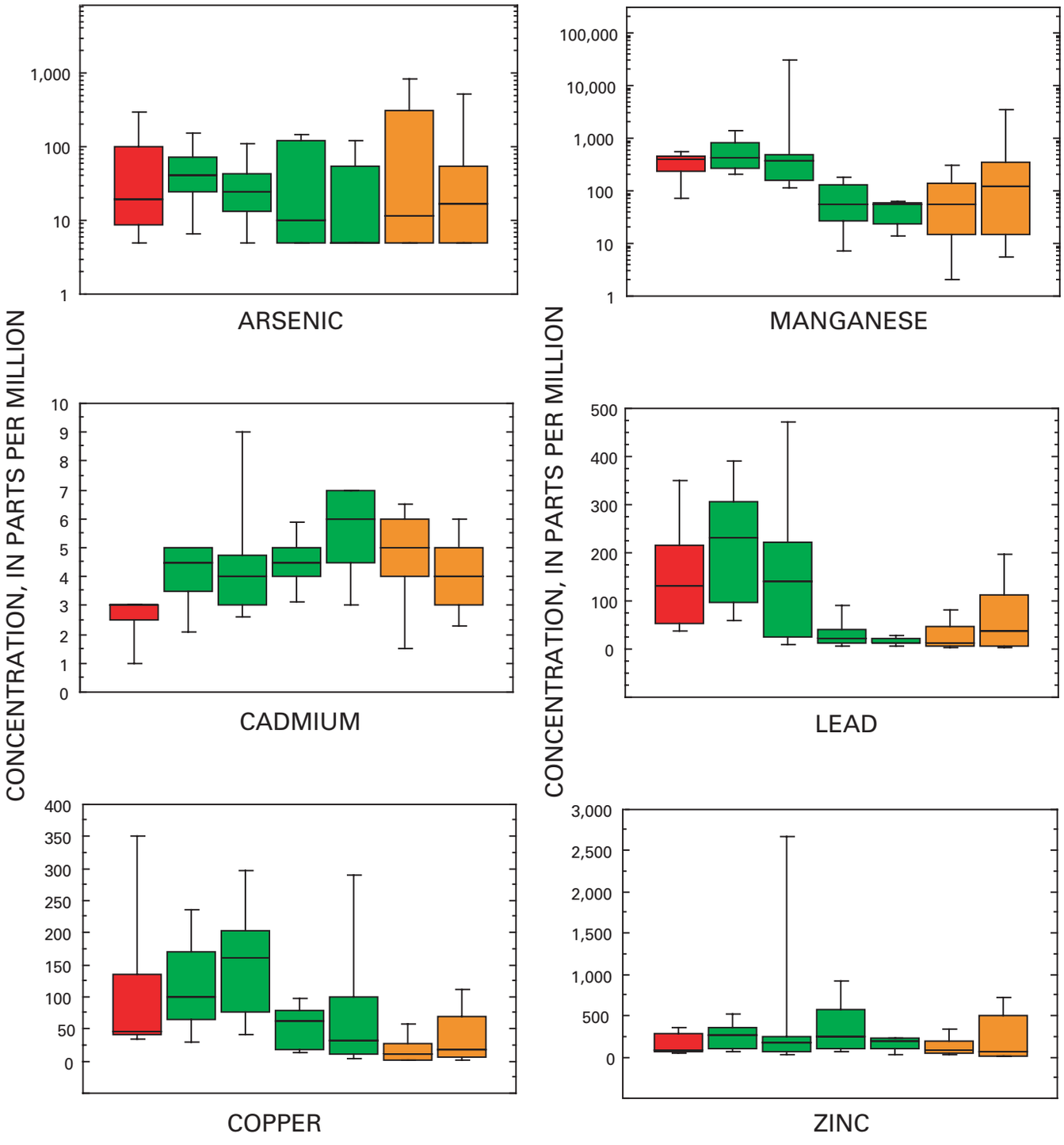

B

Figure 5 (above and facing page). Box plots showing selected solid-phase elements, grouped by mineralogy. Included are 71 out of 86 iron-cemented samples in table 2 where groups of 5 or more samples were possible. *A*, major elements in weight percent; *B*, trace elements in parts per million. Order of box plots is same as sequence in explanation.

The predominance of schwertmannite in bog iron and iron spring samples is important because optimum pH for precipitation of naturally occurring schwertmannite is between 2.8 and 4.5 (Bigham, Schwertmann, and others, 1996; Carlson and others, 2002). Hence, the presence of schwertmannite in a dated premining deposit would be evidence for acid conditions predating mining activity, as would the presence of jarosite. Schwertmannite flocculent was observed at the Silver Ledge mine portal (AMLI site # 73) with a pH of 6.1; however, this was the only known occurrence with pH >4.5 identified within the study area.

Jarosite forms in mine-drainage precipitate at a pH of 2.6, and Bigham, Schwertmann, and others (1996) have calculated a jarosite stability field for which pH <3. Although weathering halos of jarosite were commonly observed in the study area on unsaturated talus where pyrite was abundant, jarosite in ferricrete was only detected in a few localities. It was present in alternating layers with schwertmannite and goethite in two samples from the iron spring on lower Prospect Gulch (IDY00-29A and IDY00-29B; locations in table 2). Jarosite and amorphous iron oxide were primary cement minerals in a manganocrete sample from Eureka Gulch (HPDY00-16; location in table 2). Trace amounts of jarosite were also identified in an alluvial ferricrete in Browns Gulch in Mineral Creek basin (99VMS-29; location in table 2). Schwertmannite and jarosite were also identified in an augered core from an alluvial fan near peak 3,792 m described in Yager and others (2000). The relative lack of jarosite in natural ferricrete, manganocrete, and bog iron samples is attributed to few of these depositional settings having a pH less than 3.0. The lowest measured pH values were generally at mine adits, or poorly buffered seeps emerging from pyrite-bearing rocks at higher altitudes (Mast and others, this volume).

Dating of ferricrete cementation is challenging, and two approaches exist. The better approach is to find and date wood or charcoal encased in lamina of iron compounds, because the cement covering the organics must have precipitated shortly after the organic matter was deposited (an approach taken by Furniss and others, 1999). Only two such samples were obtained in our studies. A 500-year-old piece of wood (99ABFC-185D) was found encased in bog iron deposits in Dry Gulch, and a 4,500-year-old piece of charcoal (99ABFC-141A) was found encased in bog iron deposits near the top of the iron-cemented glacial outwash exposure shown in figure 6. (See Vincent and others, this volume, table 2.) Most of the ferricrete samples in this study are cemented clast-supported gravel containing little organic material. Vincent and others (this volume, fig. 7) used ^{14}C dating of encased charcoal, and stratigraphic and geomorphic relations to bracket the ages of clastic deposition, and thus constrain the age of cementation. Note that young clastic deposits had to have been cemented recently, whereas old clastic deposits could have been cemented either recently or at any time following deposition of the clasts—unless other information rules out the latter possibility. That other information includes special situations (for example, the toes of old alluvial fans) where the zone of cementation was permanently dewatered by stream incision. No such sites, however, were targeted for chemical analysis.

As discussed previously, poorly crystalline schwertmannite is considered metastable with respect to goethite (Bigham, Schwertmann, and others, 1996; Bigham, Schwertmann, and Pfab, 1996; Yu and others, 1999), and the results in figure 7 support this in general. The majority of ferricrete samples have goethite as the dominant iron-oxide mineral, and most of the host sediment was deposited prior to mining (>500 yr B.P.); the same may or may not be true for the cement. All but one of the schwertmannite samples are described as wet, and thus the ferricrete may be actively forming even if the host deposits are old. Of the 11 samples whose host deposits are less than 500 yr B.P., more than half are dominated by schwertmannite (6) or ferrihydrite (3).

Although the majority of iron-cemented samples (table 2) containing schwertmannite are coded as "wet" deposits that are usually found at stream level, at five sites schwertmannite is apparently inactive, as indicated by "dry" outcrops. Many of these dry or unsaturated deposits are potentially older than 500 yr B.P. and have been previously described as having a thinly laminated or banded texture, alternating from dark-brown to yellow bands in hand specimen (see sample pairs IDY0029A and IDY0029B, schwertmannite and jarosite, 0–10,000 years; and 99ABFC102A and 99ABFC102Ar, schwertmannite and goethite, 500–6,000 years; table 2). Alternating layers may also consist of schwertmannite and amorphous iron oxide (sample pairs 99ABFC122D1 and 99ABFC122D2, 500–4,000 years; and 99VMS65A and 99VMS65B, age unknown, table 2). More work is required to understand what these anomalously old ages represent.

The one other confirmed exception is schwertmannite identified in cemented glacial outwash in the lower reach of Cement Creek. Sample pair 99ABFC141B (schwertmannite) and 99ABFC141C (goethite) were collected in fresh exposures near the top of the iron-cemented deposit that was dated at 4,500 yr B.P. (table 2; fig. 6). The schwertmannite in this outcrop could be thousands of years old unless that sample was in an open system and water recently percolated into the sample to precipitate schwertmannite, although the sample was "dry" at the time it was collected. Another possible explanation is that the schwertmannite layer formed rapidly and was sealed off from both ground water and atmosphere by a goethite rind before complete transformation to goethite could occur. If we assume that the system is closed to circulating ground water, then iron cementation of the glacial outwash occurred following deposition when the deposit was saturated, but before Cement Creek began to incise sharply after 4,500 yr B.P. (Vincent and others, this volume) and the water table would have dropped along with the stream. Now exposed by a road cut, the massive iron-cemented outwash is perched ≈30 m

Figure 6. Iron-cemented stream gravel underlying ≥4,500-year-old bog iron containing schwertmannite and secondary goethite. Ages were determined by radiocarbon dating and geomorphological constraints, expressed as calendar years before present (cal. yr B.P.). The presence of old schwertmannite is evidence that weathering of hydrothermally altered rocks produced acid drainage thousands of years before mining occurred in the upper Animas River basin.

above the stream channel. If the system were closed, the schwertmannite may be evidence that acidic conditions were prevalent in Cement Creek thousands of years before mining occurred.

Because schwertmannite with banding is preserved in at least four deposits that are thought to be pre-modern in age, some iron-oxide minerals considered "transitional," such as ferrihydrite, schwertmannite, and jarosite, could persist in near-surface environments if shielded by a rind of goethite. Schwertmannite may be more stable in certain depositional environments and persist longer than indicated by other laboratory studies (Bigham, Schwertmann, and others, 1996; Bigham, Schwertmann, and Pfab, 1996; Yu and others, 1999). Better understanding is needed to determine the geochemical conditions necessary for preserving schwertmannite in the geologic record, especially in view of the potential value of schwertmannite, and jarosite, as indicators of pH conditions in paleo-ground water.

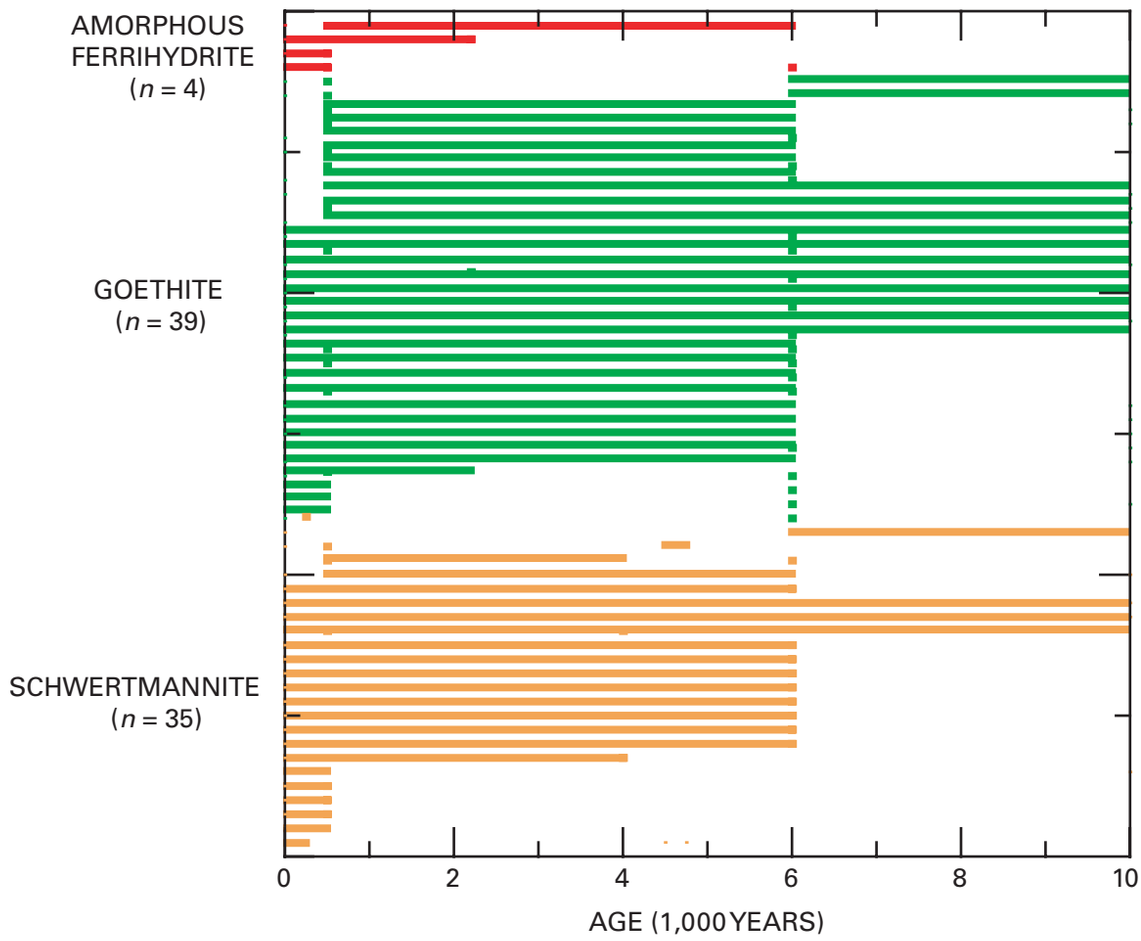

Figure 7. Histogram showing age constraints of iron-cemented deposits in Cement Creek, grouped by dominant iron-oxide mineralogy. Maximum age is age of host deposit. Range in age of iron-oxide cement is the full range indicated by the length of the bar.

Proximity to Mineral Assemblages, by Reach

Variations in solid-phase chemistry of ferricrete and manganocrete were also compared with respect to geographical proximity to exposures of acid-sulfate rock. Box plots (fig. 8) show the ranges in concentration of major and trace elements, grouped by stream reach. The stream reaches were selected on the basis of their relative abundance (or lack) of ferricrete or manganocrete.

In general, the greatest solid-phase concentrations for most trace elements were in manganocrete deposits from the headwaters of the upper Animas River. Manganocrete samples from Eureka Gulch and California Gulch contain one to four orders of magnitude more manganese (24,000–60,000 ppm) than ferricrete samples from Mineral and Cement Creeks (2–4,900 ppm) (fig. 8; Sole and others, this volume). The manganese is derived from local weathering of manganese-bearing vein gangue minerals in the Eureka Gulch area (fig. 1) (Casadevall and Ohmoto, 1977; Bove and others, this volume). Manganese is soluble at low Eh and pH conditions, but once in contact with the atmosphere, it will usually precipitate as manganese oxide at a pH ≥4.5 (Hem, 1963, 1964, 1992). Manganese oxide is known for its scavenging ability to co-precipitate with and adsorb other trace elements (Jenne, 1968, 1975; Dzombak and Morel, 1987, 1990). The greatest concentrations of cadmium (as much as 39 ppm), lead (8,000 ppm), copper (3,400 ppm), and zinc (3,800 ppm) were measured in manganocrete from the California Gulch and Eureka Gulch subbasins (n=8). Several mines and prospects are nearby, although none directly up gradient, consistent with observations that the high concentrations result from close spatial proximity to mineralized veins. In addition to trace elements shown in figure 8, high manganese concentrations in the Eureka graben area also correlate with high concentrations of beryllium (as much as 16 ppm), cerium (as much as 310 ppm), lithium (as much as 54 ppm), and silver (as much as 20 ppm). Outside of California Gulch and Eureka Gulch subbasins, two other manganese-rich ferricretes were identified in Mineral Creek basin near Chattanooga and in uppermost Cement Creek basin near the Red and Bonita mine (AMLI site # 99; Verplanck and others, this volume).

Spatial proximity to mineralized veins also accounts for the highest arsenic concentrations, ranging from 400 to 2,100 ppm, which appear as outlier values in the upper Cement Creek arsenic box plot (fig. 8). These samples were collected from bog iron deposits near the iron spring on lower Prospect Gulch. Adsorption by hydrous iron oxide is an important inorganic process that can maintain arsenic at very low levels in water (Pierce and Moore, 1980; Hem, 1992). These samples were collected directly down gradient from the Red Mountain hydrothermal alteration assemblages, which contain enargite (Cu_3AsS_4) in veins. The ground water supplying these bog iron deposits appears to circulate along fractures in the intensely altered volcanic rock (Wirt and others, 2001). Notably, these samples also contain between 350 and 1,000 ppm of vanadium (Sole and others, this volume). Like arsenic, the aqueous geochemistry of vanadium is complex, possessing three oxidation states and a low solubility under reducing conditions (Hem, 1977, 1992).

Differences in the pH of ground water do not fully account for differences in trace-element concentrations among conglomerate deposits from upper Cement Creek (pH ≤3.5) versus those in the upper Animas River tributaries (pH ≥4.5). Trace-element concentrations in ferricrete where the pH is similar to California Gulch—such as ferricrete in Mineral Creek (pH ≥4.5)—are not substantially different than those for samples from Prospect Gulch. Both Mineral and Cement Creeks, however, receive drainage from the Red Mountain and Ohio Peak–Anvil Mountain (OPAM) areas (fig. 1). Although Mineral Creek also receives drainage from the peak 3,792 altered area of Bove and others (this volume) to the west, this source produces acid drainage similar to that of the Red Mountain and OPAM areas.

The distribution and weathering of primary and secondary rock-forming minerals are fundamental in determining the distribution of manganocrete versus ferricrete, as well as the pH of ground water. Manganocrete samples generally have the largest concentrations of most major and trace elements, except for iron, sulfate, vanadium, and arsenic (fig. 8); however, this may have more to do with proximity to nearby veins than with pH, mineralogy of dominant iron species, or ferricrete subdeposit type. Within the ferricrete subdeposit types, spatial differences in ground-water pH and chemistry probably had a strong influence on the mineralogy of the dominant iron-oxide species. The deposit types, such as conglomerate-type deposits versus bog iron and spring deposits, are largely determined by the environmental setting at the location where ground water emerges at the ground surface and becomes oxidized. Although the largest differences in the distribution of major elements are most strongly associated with the ferricrete subdeposit type owing to the chemical influence of sediment clasts, differences in trace-element concentrations of copper, manganese, and lead appear to relate to pH. Differences in the concentration of arsenic, sulfate, iron, and manganese appear related to close spatial proximity to mineralized veins. For these elements, factors that are typically important in other settings, such as sorption and pH, may be secondary to availability in this highly mineralized environment. The most important factor determining the acidity and concentration of solid-phase trace elements for both ferricrete and manganocrete appears to be the underlying geology and proximity down gradient from a mineralized source area. The trace-element chemistry of ferricrete and manganocrete deposits largely predates the influence of mining, and thus may serve as a geochemical record of iron-rich or manganese-rich precipitates produced by long-term weathering of acid-sulfate and ore-bearing minerals up gradient from a given site.

Spatial Associations of Ferricrete and Bog Iron with Ground-Water pH, Geomorphology, and Alteration Assemblages

Ferricrete deposits are exposed nearly continuously along some reaches of Cement Creek and Mineral Creek (Yager and Bove, this volume, pl. 2; Vincent and others, this volume). Elsewhere, ferricrete is notably less prevalent, for example, in the middle reach of Cement Creek. Ferricrete is almost entirely absent along the Animas River upstream from the confluence with Cement Creek at Silverton, although manganocrete deposits are found in the Eureka, Placer, and California Gulch subbasins. This section describes how spatial patterns in the distribution of ferricrete and manganocrete relate to the mapped extent of acid-sulfide mineral assemblages up gradient from the deposits. Weathering of acid-sulfate minerals affects the pH and geochemistry of ground water, which in turn results in the formation of iron and manganese-oxide precipitates.

The areal extent of major mineral assemblages was calculated for selected subbasins in Cement and Mineral Creeks (table 5). The percentages used following are the areal coverage in percent of the total subbasin area. The areas covered by Quaternary alluvium were subtracted from the total area in calculating the percentage of each mineral assemblage type. The major alteration assemblages mapped for this study are the acid-sulfate (AS), quartz-sericite-pyrite (QSP), vein-related quartz-sericite-pyrite (V-QSP), and weak sericite-pyrite (WSP) rock types (Bove and others, this volume; Yager and Bove, this volume, pl. 2). Regional alteration assemblages which have undergone less intense hydrothermal alteration are referred to as propylitized (PROP) rock.

Statistical descriptions of 300 springs and streams for this study (Mast and others, this volume) indicate distinct water-quality characteristics for each mineral assemblage. For the purposes of this discussion, the water chemistry for each water type is briefly summarized here. PROP rock contains as much as 30 percent calcite, and water chemistry is controlled primarily by dissolution of calcite and some pyrite. Water samples in contact with PROP rock tend to have neutral pH (>6) and measurable alkalinity, are relatively dilute, and commonly

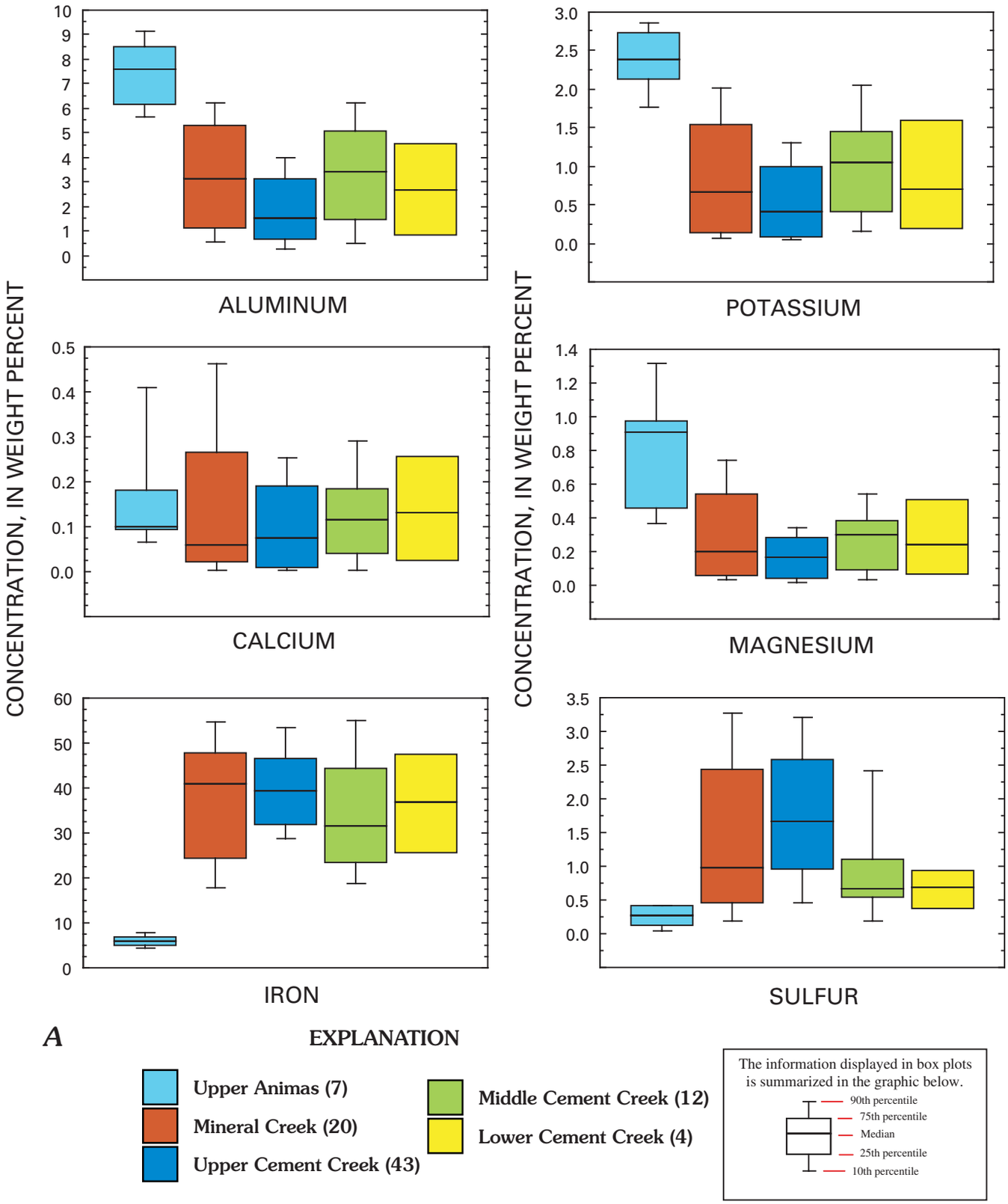
CONCENTRATION, IN WEIGHT PERCENT
ALUMINUM
POTASSIUM
CALCIUM
MAGNESIUM
IRON
SULFUR
A
EXPLANATION
Upper Animas (7)
Mineral Creek (20)
Upper Cement Creek (43)
Middle Cement Creek (12)
Lower Cement Creek (4)
The information displayed in box plots is summarized in the graphic below.
90th percentile
75th percentile
Median
25th percentile
10th percentile

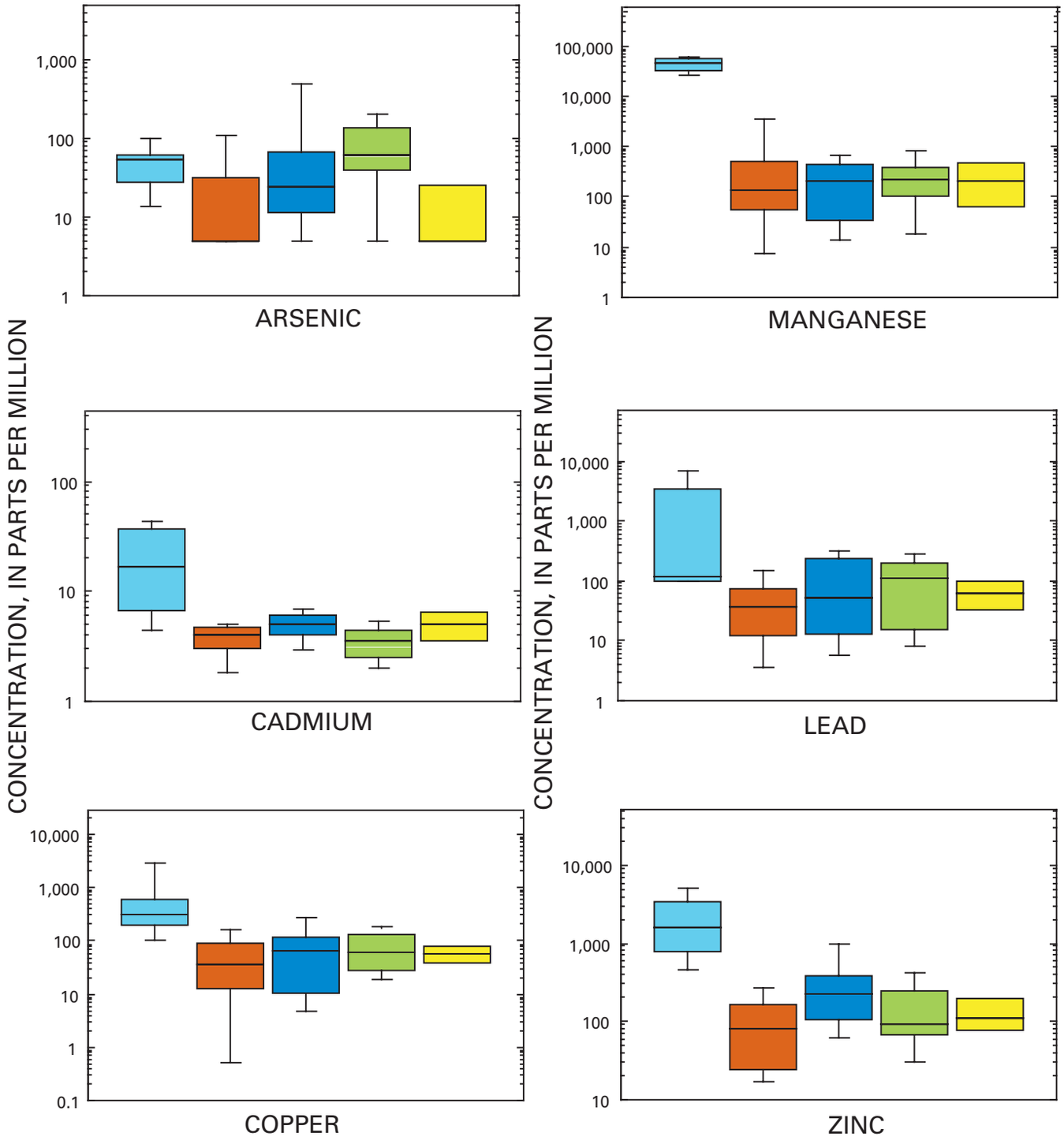

B

Figure 8 (above and facing page). Box plots showing selected solid-phase elements, grouped by stream reach. *A*, major elements in weight percent; *B*, trace elements in parts per million. Order of box plots is same as sequence in explanation.

Table 5. Mapped exposures of hydrothermal-alteration mineral assemblages (fig. 1) by subbasin, Animas River watershed study area.

[Based on data from Sole and others, this volume; blank, alteration type not present, percent (pct.) not applicable]

Basin	Area	Acid-sulfate (AS)		Quartz-sericite-pyrite (QSP)		Vein-related quartz-sericite-pyrite (V-QSP)	
	km²	km²	Pct. tot. area	km²	Pct. tot. area	km²	Pct. tot. area
Upper Cement Creek (west side):							
Prospect Gulch	3.3	0.62	18.7	0.98	29.9		
Georgia Gulch	1.3	0.01	0.5	0.01	0.7	0.07	5.5
Fairview Gulch	0.8					0.001	0.07
Middle Cement Creek (west side):							
Minnesota Gulch	1.7	0.00	0.2			0.16	9.5
Porcupine Gulch	0.8	0.04	5.5	0.09	11.6		
Ohio Gulch	1.2	0.32	26.0	0.28	22.4		
Topeka Gulch	1.4	0.17	12.3	0.23	17.0		
Niagara Gulch	2.2	0.92	41.9	0.41	18.6		
Henrietta Gulch	0.7	0.29	44.3				
Lower Cement Creek (west side):							
Unnamed south of Henrietta Gulch	0.3	0.04	14.0	0.00	1.2		
Unnamed north of Soda Gulch	0.9	0.28	31.1	0.04	4.3		
Soda Gulch	0.5			0.01	2.2		
Upper Cement Creek (east side):							
Unnamed north of Cascade Gulch	0.8					0.08	10.1
Middle Cement Creek (east side):							
Cascade Gulch	1.5					0.04	3.0
Grassy Gulch	0.4						
Unnamed south of Grassy Gulch	0.5						
Illinois Gulch	1.5					0.04	
Lower Cement Creek (east side):							
Hancock Gulch	1.8						
Unnamed south of Hancock Gulch	1.3	0.01	0.5	0.01	1.0		
Mineral Creek (Middle Fork):							
Red tributary of the Middle Fork	3.0			0.54	17.6	0.001	0.04

have trace-metal concentrations below detection. In contrast, QSP waters are highly acidic (pH <4) and have high sulfate concentrations, which result from pyrite weathering as the dominant reaction. QSP rocks commonly have >10 percent pyrite by weight. In addition, the high acidity appears to promote dissolution of calcite and aluminosilicate minerals such as kaolinite that are commonly present. Oxidized QSP water is highly saturated in ferrihydrite, causing precipitation of iron. AS-associated waters have low pH values similar to those produced in QSP exposures, but are comparatively much more dilute. Only four AS water samples were collected, and the collection sites were relatively high in elevation; thus, short travel paths with less water-rock interaction probably occurred for these samples. Water in contact with V-QSP (and in contact with PROP assemblages containing mineralized veins) is generally intermediate in pH and in concentrations of major cations and trace elements. All the water types were super-saturated in ferrihydrite, although the QSP water had the highest iron concentrations (as much as 77 mg/L). Based on this classification by Mast and others (this volume), the iron spring water presented in table 1 has the characteristics of acid-sulfate or QSP type waters, depending upon the amount of sulfate. Factors affecting variations in water chemistry include the amount of iron sulfides, grain size and degree of crystalline structure, degree of water-rock interaction, and differing redox conditions in ground water.

In the following discussion of spatial associations, we focus primarily on Cement Creek because of its extensive ferricrete exposures, and to a lesser extent on the middle reach of Mineral Creek, and on California Gulch in the headwaters of the upper Animas River.

Cement Creek

Extra attention is given to Cement Creek from Gladstone to Silverton because of the abundance of ferricrete, as well as detailed information for this reach from other studies presented in this volume. For the purposes of this chapter, we have subdivided the area into an upper, a middle, and a lower reach, referred to as the Gladstone to Fairview Gulch, Fairview Gulch to Hancock Gulch, and Hancock Gulch to Silverton

Basin	Weak sericite-pyrite (WSP)		Propylitic (PROP)		Quaternary (QU)		Altered areas mapped (less QU)	
	km²	Pct. tot. area	km²	Pct. tot. area	km²	Pct. tot. area	km²	Pct. tot. area
Upper Cement Creek (west side):								
Prospect Gulch	0.06	1.75	1.47	44.6	0.17	5.1	3.13	94.9
Georgia Gulch	0.04	3.21	1.07	80.8	0.12	9.3	1.20	90.7
Fairview Gulch	0.00	0.29	0.80	97.1	0.02	2.5	0.80	97.5
Middle Cement Creek (west side):								
Minnesota Gulch			1.51	89.0	0.02	1.2	1.67	98.8
Porcupine Gulch			0.48	59.3	0.19	23.6	0.61	76.4
Ohio Gulch			0.49	39.1	0.16	12.5	1.09	87.5
Topeka Gulch			0.93	68.9	0.03	1.8	1.33	98.2
Niagara Gulch			0.73	33.1	0.14	6.4	2.05	93.6
Henrietta Gulch			0.35	53.0	0.02	2.7	0.65	97.3
Lower Cement Creek (west side):								
Unnamed south of Henrietta Gulch			0.22	84.8			0.25	100.0
Unnamed north of Soda Gulch			0.58	64.6			0.90	100.0
Soda Gulch			0.46	97.2	0.003	0.6	0.47	99.4
Upper Cement Creek (east side):								
Unnamed north of Cascade Gulch			0.71	84.4	0.05	5.5	0.79	94.5
Middle Cement Creek (east side):								
Cascade Gulch			0.93	63.3	0.50	33.8	0.97	66.2
Grassy Gulch			0.40	98.2	0.01	1.8	0.40	98.2
Unnamed south of Grassy Gulch			0.18	38.3	0.29	61.7	0.18	38.3
Illinois Gulch			0.93	63.3	0.50	33.8	0.97	66.2
Lower Cement Creek (east side):								
Hancock Gulch	0.00	0.06	0.91	50.4	0.89	49.5	0.91	50.5
Unnamed south of Hancock Gulch	0.04	2.93	0.68	51.3	0.58	44.3	0.74	55.7
Mineral Creek:								
Red tributary of the Middle Fork	1.23	40.47	0.40	13.1	0.87	28.7	2.17	71.3

reaches. These informal subdivisions were based on the abundance (or relative lack) of exposed ferricrete as shown by Vincent and others (this volume). Mapping of surficial deposits between Gladstone and Silverton at 1:6,000 scale (Vincent and others, this volume, pl. 5) allows for a detailed consideration of spatial relations of ferricrete (1) with pH and water-chemistry data from both tributary and ground-water sources (Kimball and others, this volume), and (2) with the distribution of mineral assemblages mapped by Yager and Bove (this volume) and Bove and others (this volume). Ferricrete abundance is spatially associated with the degree of alteration and the areal extent of various acid-sulfate mineral assemblages in the tributary subbasins that supply ground water.

Upper Reach, Gladstone to Fairview Gulch

The greatest distribution of bog iron and ferricrete deposits occurs along Cement Creek from its confluence with the South Fork Cement Creek at Gladstone to the mouth of Fairview Gulch (Yager and Bove, this volume, pl. 2; Vincent and others, this volume, pl. 5). In order to characterize the hydrologic processes associated with ferricrete formation, we describe the surface-water and ground-water hydrology of this reach. Important surface-water sources contributing to Cement Creek at Gladstone include South Fork Cement Creek, discharge from the treatment system for Sunnyside mine (AMLI site # 96), and North Fork and mainstem of Cement Creek (fig. 9). At present, roughly half of Cement Creek's discharge at Gladstone is released from the Sunnyside mine treatment system during summer months. Treated effluent includes adit flow from the American tunnel combined with stream water from both the headwaters of Cement Creek and the North Fork. The pH of the treated flow is neutral (>6.5; neutralized with lime; Besser and others, this volume, Chapter D), whereas the pH of untreated flow during the remainder of the year ranges from 3.5 to 4.5 (Wright, Simon, and others, this volume, Chapter E10). South Fork contributes an approximately equal volume of flow with a pH between 3.5 and 4.5 (≈90 L/s in September 1996; Kimball and others, this volume). Large seasonal variations in stream quality occur in response to the accumulation of a deep seasonal snow pack and the annual hydrologic cycle (Leib and others, 2003; Wirt

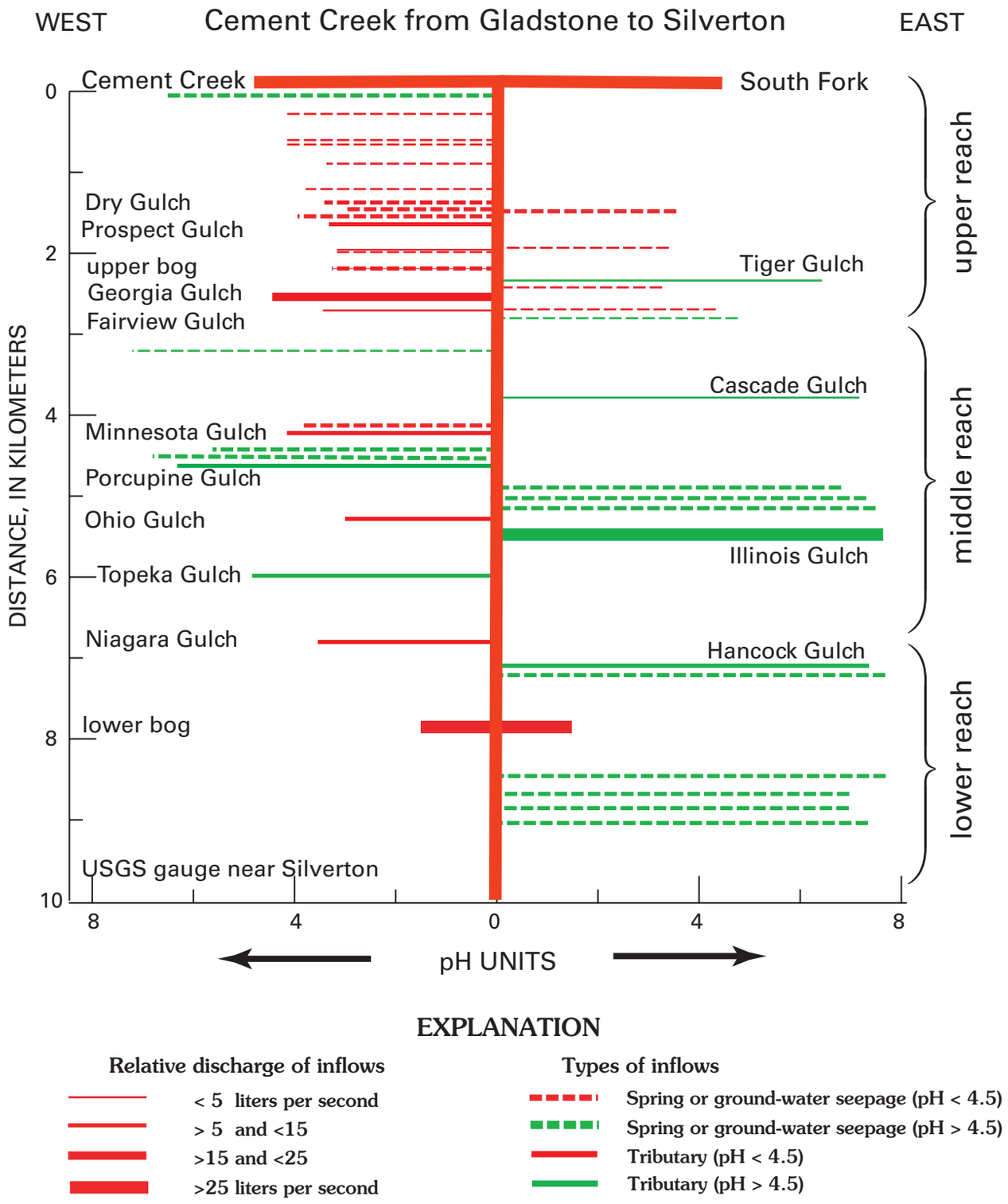

Figure 9. Schematic diagram of inflow discharge and pH from tributaries and ground water in the upper, middle, and lower reaches of Cement Creek during low-flow conditions.

and others, 2000). Iron cementation of the exposed stream banks from Gladstone to Fairview Gulch is nearly continuous (Vincent and others, this volume, pl. 5), and stream cobbles are coated or stained with iron oxides.

Between Gladstone and Fairview Gulch (fig. 9), discharge increased more than 70 percent from about 180 to 310 L/s, as measured during low-flow conditions in September 1996 by Kimball and others (this volume). Three-fourths of this 130 L/s gain is attributed to small, diffuse ground-water sources and overland flow from sedge wetlands. Contributions from three tributaries, Georgia Gulch, Prospect Gulch, and Tiger Gulch, account for the remaining 30 L/s (fig. 9).

Sedge wetlands cover most of the low-lying flood-plain and stream-terrace deposits throughout the reach, interrupted only by alluvial fans emanating from major tributaries. The sedge wetlands, discharging acidic waters, are elevated above the stream channel, generally by a meter or so. Diffuse ground water predominantly originates from the sides of the valley, as opposed to flowing parallel to the stream through gravel deposits in the center of the valley (Vincent and others, this volume). Cement Creek generally flows from north to south, but the Gladstone to Fairview reach curves from the east to the southwest, receiving most of its drainage from the west rather than from the east, as evidenced by the larger number of tributaries and larger drainage area (figs. 1 and 9). Eighty to ninety percent of the areal extent of the wetlands is on the west side of Cement Creek. Dry ferricrete deposits are exposed in stream cuts on both sides of Cement Creek, but this does not necessarily indicate the source-direction of water that formed those precipitates, because the lateral position of the creek at the time of precipitation is not known. "Wet" ferricrete (field exposures that were wet) was observed on both stream banks, but predominantly on the west bank. These observations indicate that the source of iron and acidity is mostly from the west side, down slope from the Red Mountain hydrothermal altered area (fig. 1).

In the Gladstone to Fairview reach, the areal extent of QSP, AS, and WSP assemblages is much greater west of Cement Creek than on the east. The dominant acid-producing mineral assemblages in the Prospect Gulch subbasin include about 30, 19, and 1.8 percent of QSP, AS, and WSP rock exposures, respectively—roughly half of the surface area of the Prospect Gulch subbasin. In contrast, the unnamed subbasin on the east side of Cement Creek (fig. 1 and table 5, subbasin north of Cascade Gulch and upstream of Fairview Gulch) has only about 10 percent of its area mapped as V-QSP. Propylitized rock (PROP) that underwent a less intense regional alteration underlies about 90 percent of this unnamed subbasin. Rock on the east side of Cement Creek provides considerably more acid-neutralizing capacity than rock exposed on the west side of this reach (Desborough and Yager, 2000).

The pH of wetlands, bog iron deposits, seeps, and springs in this reach is highly variable, but predominantly acidic. At the interface between a sedge wetland and iron bog, one can measure many different pH values ranging from 3.2 to 6.8—all within a distance of just a few meters (Yager and Bove, this volume, pl. 2, fig. 14). Most of the ground water entering Cement Creek, however, has low pH. Twenty-three inflows sampled during the 1996 tracer study had a mean pH of 3.7, which accounts for the decrease in pH from 6.5 to 4.0 from Gladstone to Fairview Gulch (Kimball and others, this volume). The near-surface values for dissolved oxygen in wetland areas also tended to be highly variable, ranging from about 0.1 to 7 mg/L. Specific conductance was also highly variable: measurements of various sedge wetlands, iron bogs, and iron seeps and springs ranged between 89 and 1,100 µS/cm (microsiemens per centimeter). The large spatial variations in these field parameters indicate that the wetlands and permeable host sediment served as mixing zones between the deeper circulating, low-pH ground water and either the atmosphere or relatively shallow, more oxygenated water.

The upper reach has several examples of iron precipitating where ground-water flow emerges from fractured bedrock. Near the mouth of Fairview Gulch, two springs, one on each bank, are aligned along the trend of a prominent fault or fracture system that intersects Cement Creek (Yager and Bove, this volume, pl. 1). Another example of acidic water emerging from fractures in bedrock is the iron spring in lower Prospect Gulch, which is located at a break in slope at the base of a pronounced linear feature in the topography (fig. 10; Wirt and others, 2001). The pH for all three of these iron-precipitating, fracture-controlled springs is between 2.9 and 3.5.

Fracture flow is the likely source of the many low-pH inflows in this reach. For 12 iron-rich springs sampled in this reach (tables 1 and 6), pH ranged from 3.2 to 4.6, specific conductance ranged from 523 to 1,800 µS/cm, and dissolved sulfate concentrations ranged from 240 to 1,000 mg/L. In contrast, Tiger Gulch, a dilute tributary inflow, had a pH value of 6.4, specific conductance of 90 µS/cm, 23 mg/L of sulfate, and 12 mg/L of bicarbonate. These dilute inflows have little acid-neutralizing capacity and react quickly, having little effect on the water quality of Cement Creek or other acid-sulfate waters. Exposures of fractures that carry acidic ground water are typically concealed by colluvium and stream-terrace deposits. In addition, many colluvial and alluvial deposits are cemented with ferricrete or covered with sedge wetlands. Precise directions of ground-water flow paths are poorly constrained. In general, ground water flows from the mountains towards the center of the valley, and then down the center of the valley beneath and adjacent to Cement Creek.

Ferricrete and bog iron are actively forming at many iron springs and bogs, and numerous streambank locations in the upper reach of Cement Creek. This is further indicated by the frequency of mapped occurrences of wet ferricrete along the exposed stream channel (Vincent and others, this volume, fig. 6). In addition, ferricrete forms on the bottom and sides of Cement Creek in gaining reaches, although the rates and volumes of deposition are variable and difficult to measure. Loose reddish- or orange-brown flocculent is present on the stream bottom and coats stream cobbles in many locations, although the fine-grained flocculent tends to be washed away at higher flows. Desborough and others (2000) observed

Figure 10. Fracture-controlled iron spring in lower Prospect Gulch.

orange-brown precipitates (ferrihydrite and schwertmannite, as determined by X-ray diffraction) accreting onto a wooden stake that was left in the gaining reach upstream from Tiger Gulch and Georgia Gulch for several weeks, although the stake never became firmly cemented to the substrate. In this study, we placed a 2-in. diameter metal pipe in the stream and anchored it in place on the bed with angular rocks. During a 3-year period, no cementation of the pipe or the rock holding it on the streambed took place.

The streambed is strongly cemented, however, in the gaining reach between the upper bog and Tiger Gulch and Georgia Gulch, where two large, opposing alluvial fans cause Cement Creek and associated flood-plain deposits to narrow (fig. 11). Numerous iron-rich seeps, resulting from the shallow water table and an abrupt change in stream gradient, occur on both sides of the channel upstream and downstream from the two fans near their interface with lateral stream terraces. Freshly precipitated cement, coating the sides and bottom of the stream, is modifying the channel from year to year. This seemed an ideal location to sample actively forming ferricrete within the channel.

Using a sledgehammer, we collected cement beneath the water from the bottom and sides of the stream channel near the upper bog. Chemical analyses and X-ray diffraction of strongly cemented sections of the low-flow streambed (fig. 11; sample 00ABFC-231 in table 2) indicate that precipitate is composed of at least 50 percent iron-oxide minerals and one-third crystobalite (amorphous quartz). Crystobalite is supersaturated in nearly all of the iron-rich ground water sampled (table 4), and precipitates along with the iron-oxide minerals under similar geochemical conditions. Ferricrete with a high content of crystobalite is more resistant to mechanical erosion and in this case forms small stairstep-sized waterfalls at several locations in the upper reach. The rate at which the ferricrete is accumulating is unknown, although the stream incised to its present level about 500 years ago, placing a maximum constraint on the age of the deposit.

Middle Reach, Fairview Gulch to Hancock Gulch

In contrast with the Gladstone to Fairview Gulch reach, relatively few ferricrete deposits occur between Fairview Gulch and Hancock Gulch (Vincent and others, this volume, pl. 5). This relative absence is largely attributed to a greater percentage of surface runoff from the east side of the Cement Creek basin that is dominated by weakly propylitized volcanic rock (Bove and others, this volume), resulting in a higher pH for many of the tributary and ground-water inflows.

Table 6. Characteristics of selected stream reaches with respect to abundance of ferricrete.

Reach	Subreach	Selected inflows	Relative abundance of ferricrete	Discharge liters/s[1]	Major mineral assemblages[2]	Base flow pH	Sulfate concentration (mg/L)[3]
Cement Creek							
	Upper (Gladstone to Fairview)		Continuous	180–310	mixed	4.0–6.5 (sometimes treated)	410–500
		Iron springs (12)	Continuous	diffuse	QSP/AS	3.2–4.6	240–1,000
		Tiger Gulch	None	3.1	PROP	6.4	23
		Adits in Prospect Gulch (3)	Not determined	<1	mine affected	2.5–4.1	83–1,100
	Middle (Fairview to Niagara)		Intermittent	310–600	mixed		
		West side tributaries (5)	Intermittent	9.7–13.5	AS/QSP/PROP	3.0–4.9	147–600
		East side tributaries (4)	None		PROP	6.8–7.6	30–56
		Mine adits (3)	Not determined	>50 E	mine affected	5.7–7.3	530–870
	Lower (Niagara to Silverton)		Continuous	600–700	mixed	3.7	150–480
		Lower bog	Continuous	50	AS/QSP	3.0	550
		Inflows near Hancock (2)	None	30	PROP/landslide	7.3–7.6	29–53
Mineral Creek							
	Middle Fork to South Fork		Continuous	21–32.5	AS/QSP	5.7–4.9	134–220
		Middle Fork	Continuous	18.1	AS/QSP	4.7	290
		Small seeps	Continuous	diffuse	AS/QSP	3.6–5.0	56–390
Upper Animas							
	California Gulch to mixing cascade		No ferricrete; manganocrete is abundant	5.0–50	PROP/AS	5.2–7.0	125–175
		Small seeps		diffuse	vein PROP	4.3–5.3	150–470

[1]Data from Kimball and others (this volume, Chapter E9).

[2]QSP, quartz-sericite-pyrite; AS, acid-sulfate; PROP, propylitic.

[3]Data in Sole and others (this volume, Chapter G).

Through this reach, low-flow discharge doubled from approximately 310 L/s to 607 L/s (Kimball and others, this volume). At least 110 L/s of this gain came from seeps, springs, and tributaries on the west side of the valley. About 65 L/s was attributed to visible sources on the east side, and 48 L/s could not be attributed to any observed source. On the west side, Minnesota, Porcupine, Ohio, Topeka, and Niagara tributaries each contributed between 9.7 and 13.5 L/s, and the Elk tunnel (AMLI site # 147) and Anglo-Saxon mine (AMLI site # 183) adits contributed about 15 and 14 L/s, respectively. The mean pH for these five west-bank tributaries was 4.4, and the pH of the three mine inflows ranged from 5.7 to 7.3 (fig. 9). Despite the relatively high pH of the mine-related inflows, sulfate concentrations were high (760–868 mg/L). In contrast, several inflows draining propylitic rock on the east side of Cement Creek had a mean pH value of 7.3 and mean sulfate concentration of 35 mg/L (Cascade Gulch, two large seeps, and a large unnamed spring draining a glacial moraine deposit upstream from Ohio Gulch). Illinois Gulch (which includes a large contribution from the Yukon tunnel; AMLI site # 186) contributed the most inflow at 33 L/s, having a pH of 7.6 and 533 mg/L sulfate. The pH of Cement Creek decreased slightly from about 4.0 to 3.8 from Ohio Gulch to Niagara Gulch (Kimball and others, this volume).

Most volcanic rock east of Cement Creek is propylitically altered, consisting of quartz, chlorite, epidote, and calcite (plus or minus plagioclase, amphibole, biotite, and opaque oxides)—but little pyrite, except for that associated with veins or finely disseminated. This mineral assemblage represents an early regional alteration event that was largely unaffected by the subsequent acid-sulfate altering fluids in the Red Mountain area (Bove and others, 2001; Bove and others, this volume). At high elevations some remnants of primary mineral assemblages are still preserved, including plagioclase, quartz, amphibole, and some biotite. The pH of springs in contact with propylitized rock tended to be neutral (>5) in contrast with low-pH background water (<5) draining more intensely altered, pyrite-bearing rock (Mast and others, this volume). Propylitically altered rock also occurs on the west side of Cement Creek south of the Red Mountain hydrothermal altered area (fig. 1).

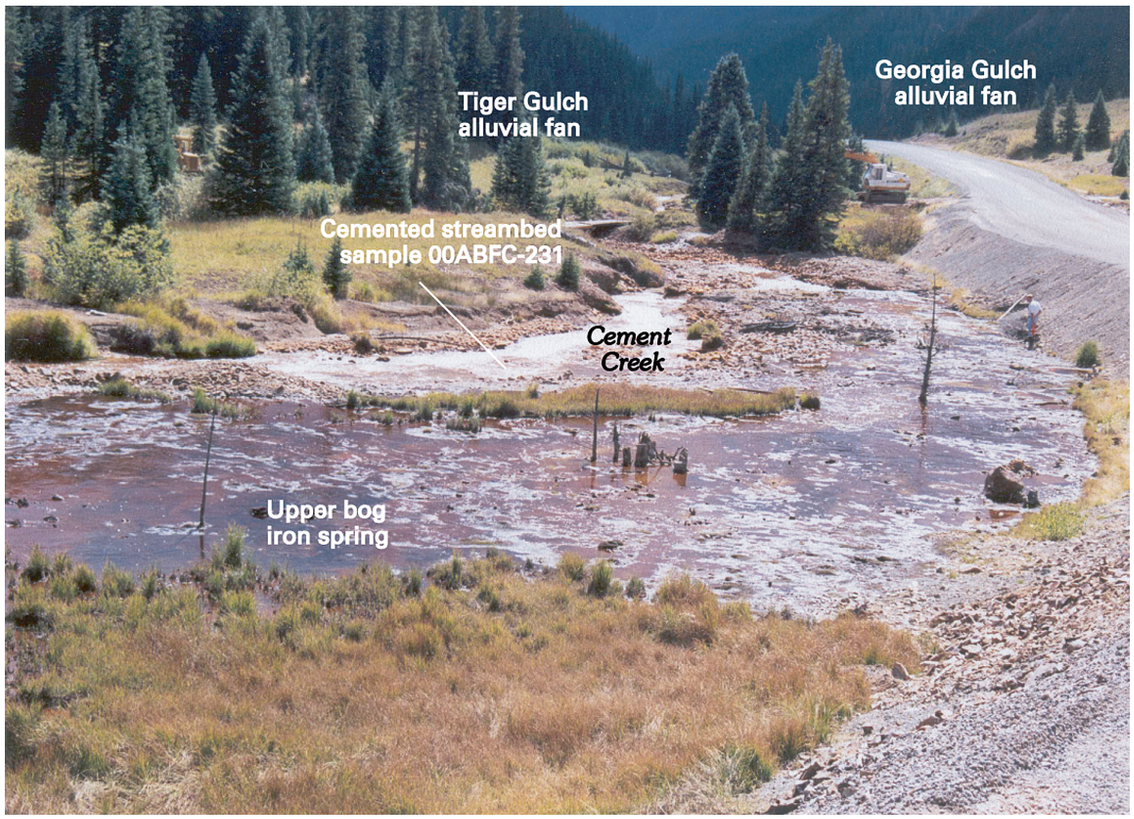

Figure 11. Gaining reach of Cement Creek (left channel) near upper bog (foreground), characterized by numerous iron-rich seeps. View is downstream toward Georgia Gulch and Tiger Gulch alluvial fans (background). Streambed of Cement Creek adjacent to upper bog is cemented with ferricrete.

The Georgia, Fairview, and Minnesota Gulch subbasins have <10 percent of AS and QSP alteration types, although V-QSP is locally important in Minnesota Gulch.

Farther south, subbasins draining the Ohio Peak–Anvil Mountain hydrothermal altered area (Porcupine, Ohio, Topeka, and Niagara subbasins) have between 17 and 60 percent acid-generating rock types exposed (table 5). High-elevation colluvial ferricrete is present in the Topeka and Niagara subbasins, as well as bog iron in upper Topeka Gulch. The AS and QSP alteration assemblages in the OPAM area are similar to those in the Red Mountain area, although the OPAM area tends to be lower in the concentrations of copper, lead, arsenic, and other trace elements (Bove and others, this volume). The Ohio, Niagara, and Henrietta subbasins have more acid-sulfate alteration in comparison to Prospect Gulch—with 26 to 44 percent exposures of AS (table 5). In addition, Porcupine, Ohio, Topeka, and Niagara subbasins contained from 12 to 22 percent exposures of QSP. These mineral assemblages are highly friable and tend to be easily eroded, as evidenced by the large alluvial fan at the mouth of Ohio Gulch (Vincent and others, this volume).

The lower abundance of ferricrete deposits in this reach is attributed to higher pH for most tributary inflows (fig. 9), and a larger fraction of inflow from propylitically altered subbasins relative to the upper reach (table 5). The middle reach also receives proportionately more inflow from perennial tributaries and less from ground-water discharge (roughly 15 percent of new water for the middle reach versus 75 percent for the upper reach). There are distinct differences in the pH of water on different sides of the valley, with the east-side inflows relatively neutral (6.8–7.6; table 6), and the west-side inflows more acidic (mean=4.4). The two subbasin inflows with the largest areal extent of AS and QSP mineral assemblages—Ohio Gulch and Niagara Gulch—had pH values of 3.0 and 3.6, respectively. A corresponding decrease in the pH of Cement Creek from about 4.0 to 3.8 occurs between these two tributaries, and ferricrete deposits are present along the channel near Niagara Gulch.

Lower Reach, Hancock Gulch to Cement Creek Gauge near Silverton

Ferricrete deposits are exposed almost continuously along the lower reach of Cement Creek from the mouth of Hancock Gulch downstream to the Cement Creek gauge near Silverton. Low-flow discharge in September 1996 increased from about 600 to 700 L/s (Kimball and others, this volume).

The mean stream pH for the reach is 3.7. The greatest tributary inflows—Hancock Gulch and an unnamed subbasin to the south—contributed a net inflow of ≈30 L/s with pH values of 7.3 and 7.6, respectively. The source area for these inflows is along the base of a large landslide deposit east of Cement Creek (Blair and others, 2002; Vincent and others, this volume). The greatest ground water inflow (50 L/s) is in the vicinity of the lower bog on Cement Creek (figs. 1, 9), which had a pH measurement of 3.0.

Discharge from the lower bog includes diffuse inflow from wetlands on both banks, just downstream from an old railroad trestle. A small prospect along an altered vein zone could have some impact on the water quality of the wetland system. The alteration zone is a prominent feature in geophysical data (Smith and others, this volume, Chapter E4). Ground water supplying the wetland is likely derived from a large fracture system; however, evidence of ground water emerging from fractured rock is concealed by steep forested terrain on the west bank and by landslide debris on the east bank of Cement Creek.

Hydrothermal alteration in the lower reach is considerably less than that of upstream reaches of Cement Creek. Hancock Gulch and the unnamed tributary directly south, for example, contain little AS or QSP, as does Soda Gulch on the west side. The largest exposure of acid-generating rock occurs on the west side in an unnamed subbasin north of Soda Gulch. This unnamed tributary, with 31 and 4.3 percent AS and QSP exposures, respectively, drains the east flank of Anvil Mountain and joins Cement Creek near the lower bog. Where alteration does occur, at least one or more small prospects have been developed on either side of this reach. Wet ferricrete exposed in channel banks is present where the lower bog enters Cement Creek. Because the lower bog merges with Cement Creek so far downstream, this source has proportionately less influence on stream pH and chemistry than if it were located farther upstream, owing to dilution effects (Kimball and others, this volume). Cementation of streambed clasts through most of this reach is attributed to mixing of the low-pH and iron-rich ground water from the lower bog with more oxygen-rich water in the stream and underlying hyporheic zone.

Mineral Creek between Middle Fork and South Fork

Ferricrete is exposed continuously along Mineral Creek between its Middle and South Fork tributaries (Yager and Bove, this volume, pl. 2). Water chemistry in this reach is dominated by low-pH water from Middle Fork Mineral Creek, although small, acidic, iron-rich springs discharge from both banks through this reach. Discharge from Mineral Creek and from Middle Fork Mineral Creek was roughly equal during low-flow conditions (20.6 and 18.1 L/s, respectively, September 14, 1996; Kimball and others, this volume). Middle Fork Mineral Creek had a total-recoverable iron concentration of nearly 40 mg/L with a pH of 4.7. The addition of Middle Fork Mineral Creek to the mainstem caused pH to decrease from 5.7 to 4.8, whereas total recoverable iron increased more than three-fold in Mineral Creek, from 1.5 to 5 mg/L. The slight gain of 5 L/s between the Middle and South Fork Mineral Creek tributaries is attributed to small acidic springs, which have little effect on in-stream chemistry or trace-metal loads. We attribute the acidic nature of these small inflows to large exposures of altered rock on both sides of Mineral Creek. The subeconomic porphyry copper-molybdenum deposit of peak 3,792 m is west of this reach and the OPAM area is east (Bove and others, this volume). Bog iron deposits occur nearly continuously along both banks. In-stream pH and iron concentrations remain fairly constant throughout this reach to the mouth of South Fork Mineral Creek. Inflow from South Fork is neutral (7.2), and the pH downstream from its confluence is 6.8 during low-flow conditions. The distribution of ferricrete deposits is no longer continuous downstream from the mouth of South Fork Mineral Creek.

Middle Fork Mineral Creek contributes the greatest loads of aluminum, iron, manganese, and sulfate to Mineral Creek (Kimball and others, this volume). The loads are derived from weathering of QSP alteration assemblages surrounding the subeconomic porphyry copper-molybdenum deposit at peak 3,792 m and from mining (Mast and others, this volume). An unnamed north-flowing tributary subbasin, the major tributary inflow to Middle Fork Mineral Creek, has about 18 and 40 percent areal extent of QSP and WSP rock types, respectively (table 5). Ferricrete is present along the QSP and WSP reaches of the tributary, which contributes about 20 percent of the zinc load and 24 percent of the copper load to Middle Fork Mineral Creek (Mast and others, this volume). Mast and others have estimated that comparable loads of zinc (24 percent) and copper (19 percent) can be attributed to mining-related sources elsewhere in the Middle Fork Mineral Creek basin.

California Gulch, a Headwater Tributary of the Upper Animas River

Springs and streams in the east half of the study area, drained by the upper Animas River upstream of Silverton, are substantially higher in pH (generally >6.5; Mast and others, this volume; Wright, Simon, and others, this volume), and ferricrete deposits and bog iron are correspondingly sparse (Yager and Bove, this volume, pl. 2). The neutral pH is attributed to the presence of carbonate minerals in the propylitically altered rocks throughout most of this basin. In several locations, alluvial deposits are cemented with blue-black manganese-oxide cement, here referred to as manganocrete (Verplanck and others, this volume; Yager and Bove, this volume, pl. 2). Similar to ferricrete in their genesis, these sedimentary conglomerates are less abundant than the iron-cemented deposits in Mineral and Cement Creeks, occurring along the flanks

of California and Houghton Mountains (in the California, Placer, and Eureka Gulch subbasins, fig. 1) and as black rock varnish forming a surficial coating on stream cobbles and cementing historical gravel deposits below the old mining and milling town of Eureka (Vincent and Elliott, this volume, Chapter E22). The cement coatings are derived from the weathering of manganese-rich vein minerals in the Eureka graben area described by Casadevall and Ohmoto (1977) and also from mill tailings derived from ore production that were discharged to the Animas River at Eureka.

Naturally occurring manganese-rich springs were sampled along the lower end of manganocrete-cemented alluvial fans flanking the north side of California Mountain, in this study and also by Kimball and others (this volume). These springs are low in dissolved oxygen, range in pH from 4.3 to 4.8, and have higher concentrations of dissolved sulfate, manganese, iron, and aluminum than the adjacent downstream reach of California Gulch (Kimball and others, this volume). Manganese springs (see samples 99VAF01, MN-1, and CGS, table 1) had among the greatest concentrations of dissolved aluminum (as much as 24 ppm), copper (as much as 4.6 ppm), and zinc (as much as 14 ppm). For further information on manganese-oxide precipitates, see Hem (1963, 1964), Carpenter and Hayes (1980), Robinson (1993), Stollenwerk (1994), and Lind and Hem (1993).

Trace-Element Content of Naturally Occurring Acid-Sulfate Ground Water as a Geochemical Baseline for Mine-Affected Drainage

Successful remediation strategies for acidic mine drainage require a detailed understanding of mineralization and hydrology surrounding the mines in order that realistic geochemical baselines for water quality can be developed. The term "baseline" is used herein to refer to water that is unaffected by mining, milling, or weathering of excavated waste rock. We propose that for the Animas River watershed study area the acidic ground water associated with ferricrete, bog iron, and manganocrete deposits serves as an aqueous-phase analog for ground water affected by acidic mine drainage. Acid-sulfate-type ground water bearing high concentrations of iron and manganese represents extreme near-surface conditions, and these are among the worst-case concentrations that could be expected from the weathering of a mineral deposit. The acid-sulfate-type water serves as a geochemical baseline for what undiluted ground water draining a mineral deposit may have been like prior to mining.

In a typical stream, water at any given point is a composite of ground water and surface-water runoff from a variety of sources, and thus a contribution of acid-sulfate-type ground water would almost always be diluted by other contributions. The spring water sampled in this study therefore represents a bias toward the extreme end and should not be used to set remediation goals for surface-water streams.

In figure 12, the sum of most common trace elements (zinc, copper, cobalt, and nickel in µg/L), or "sum of metals" is plotted against pH for different types of water that were collected throughout the Animas River watershed study area. The upper graph (*A*) shows the range of results for ground-water, spring, and seep samples from the project database (Sole and others, this volume). Sample descriptions indicate that these samples were not obviously affected by mining activity. Base flow during late-summer conditions from tributaries, largely from the tracer studies by Kimball and others (this volume), is also plotted, although many of the samples in this group are from subbasins where mining occurred, and are likely affected by historical mining to some degree. Both ground-water and base-flow tributary samples plot across a wide range of pH, with trace-element concentrations reflecting a wide range of conditions, from springs fed by dilute snowmelt to older ground water with as much as 1,200 µg/L for sum-of-metals concentration. The upper graph (*A*) provides a watershed-scale picture covering a broad range of pH and sum-of-metal conditions that were sampled in the duration of the 5-year investigation by the numerous coworkers on the project. The lower graph (*B*) compares iron-rich ground water collected in this study (table 1) with mine-affected samples from the project database (Sole and others, this volume). In accordance with the criteria of Mast and others (this volume), the iron-rich ground water samples in graph *B* are not significantly impacted by mining activities. In contrast, the acidity and sum-of-metal content of the naturally occurring iron-rich water are exceeded by a majority—although not all—of the database samples coded as affected by mining. The lower graph (*B*) gives us a clear indication of how the most extreme mine-affected samples compare with the most extreme ground water from unmined areas strongly affected by weathering of acid-sulfate rock (this study, table 1). Based on the lower graph, a reasonable geochemical baseline for acid-sulfate-type ground water from the Animas River watershed study area is the maximum concentration of the sum of metals (Co, Cu, Ni, and Zn) for the iron-rich ground water. A reasonable sum-of-metals limit for a ground-water discharge leaving a mine-affected site (an extreme condition) could be set at 1,200 µg/L for this study area—a hydrothermally altered Tertiary-age volcanic rock that has naturally weathered in a temperate alpine setting. Limits for selected trace-element concentrations that are of particular concern to aquatic life and human health, such as copper and zinc, can be determined in a similar fashion. In upper Cement Creek, the maximum values measured for iron-rich ground water were 0.080 µg/L copper and 1,500 µg/L zinc (table 1). Local guidelines could be developed on a site-by-site basis for a given reach, depending on the hydrologic setting and degree of hydrothermal alteration.

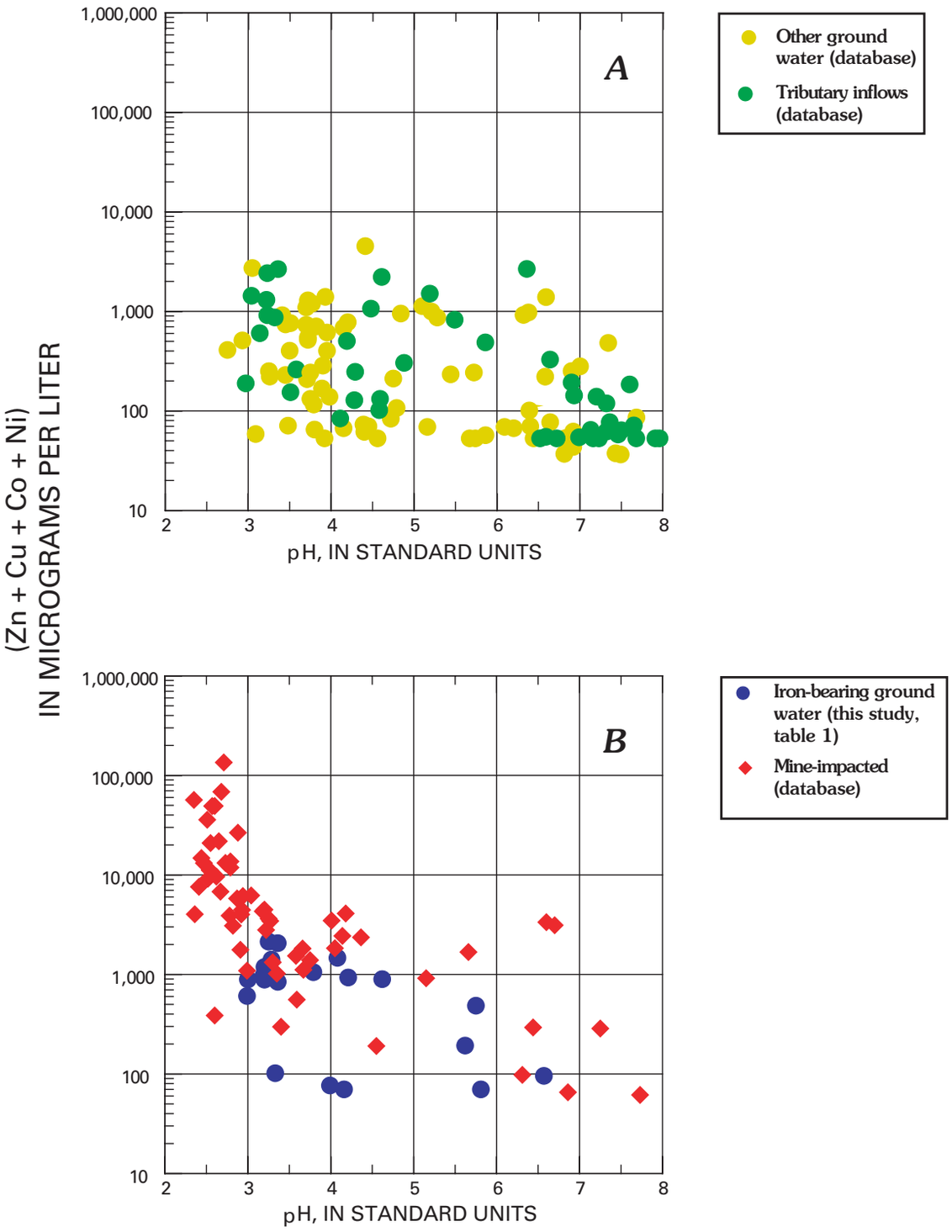

Figure 12. Sum of trace metals (Zn+Co+Cu+Ni), versus pH for *A*, ground-water and tributary inflows, and *B*, iron-rich ground water (this study) compared with mine-affected samples. Metals data include both filtered and unfiltered water samples from database (Sole and others, this volume). Note log scale on *y*-axis.

Conclusions

Comparison of ground-water pH conditions in the Animas River watershed study area with mapped occurrences of ferricrete indicates that active ferricrete and bog iron deposits are most likely found in areas where ground-water pH is consistently less than 4.5. An exception to this finding is that older, inactive ferricrete and bog iron deposits are locally preserved above modern stream terraces (and the present-day water table), such as the cemented paleo-stream gravel deposits in Cement and Mineral Creeks. The greatest sources of acid-sulfate water are the Red Mountain and OPAM areas draining east to Cement Creek and west to Mineral Creek, and the area surrounding the unnamed peak 3,792 m between Middle Fork and South Fork Mineral Creek (fig. 1). The alteration assemblages most commonly associated with acid drainage are the acid-sulfate, quartz-sericite-pyrite, V-QSP, and weak sericite-pyrite alteration zones. Ferricrete occurs extensively along the valley floors and banks of Cement Creek and Mineral Creek, directly down gradient from the greatest occurrences of acid-generating rock types. The aqueous and solid-phase chemistry of ferricrete environments can be used as a geochemical baseline for an extreme but natural condition—acid-sulfate-type ground water draining hydrothermally altered volcanic rock in a given climatic setting.

In this chapter we have investigated aqueous chemistry of ground water in contact with ferricrete deposits, evaluated solid-phase chemistry and mineralogy of ferricrete deposits, and considered spatial relations with altered mineral assemblages and typical environments of ferricrete and bog iron deposition. Lastly, we have developed geochemical baselines for major and trace elements in a most extreme, but natural condition—that of acid-sulfate-type ground water unaffected by mining in close proximity to hydrothermally altered mineral assemblages. The hydrologic processes, mineralogy, and major-element chemistry governing the formation of ferricrete have many analogies to the formation of iron precipitates resulting from acidic mine drainage. The prevalence of schwertmannite in a wide range of sedimentary deposits down gradient from acid-sulfate rock assemblages is evidence that pH of ground water in these localities was probably between about 3.5 and 4.5 before mining began.

Despite the poor quality of these naturally occurring acid-sulfate-type ground waters, mine-affected water samples are commonly even more acidic with higher trace element concentrations, some by as much as two orders of magnitude (fig. 12). The most heavily mine affected water samples have pH <3, which increases the solubility of iron, aluminum, and most trace elements such as zinc, copper, nickel, cobalt, and arsenic, resulting in sum-of-metals concentrations that commonly exceed 1,200 µg/L. Representative sampling of ferricrete deposits and acid-sulfate ground water provides a needed strategy for our understanding of worst-case water-quality conditions that are natural in origin. The water chemistry of iron- and manganese-rich springs can be used as a premining baseline of pH and trace-element concentrations in ground water adjacent to mined deposits.

References Cited

Ball, J.W., and Nordstrom, D.K., 1991, WATEQ4F—User's manual with revised thermodynamic database and test cases for calculating speciation of major, trace, and redox elements in natural waters: U.S. Geological Survey Open-File Report 90–129, 185 p.

Bassett, R.L., Miller, W.R., and McHugh, J.B., 1992, Simulation of natural acid sulfate weathering in an alpine watershed: Water Resources Research, v. 28, p. 2197–2209.

Bigham, J.M., Carlson, L., and Murad, E., 1994, Schwertmannite, a new iron oxyhydroxy-sulphate from Pyhasalmi, Finland and other localities: Mineralogical Magazine, December 1994, v. 58, p. 641–648.

Bigham, J.M., Schwertmann, Udo, Carlson, L., and Murad, E., 1990, A poorly crystallized oxyhydroxysulfate of iron formed by bacterial oxidation of Fe (II) in acid mine waters: Geochimica et Cosmochimica Acta, v. 54, 2743–2758.

Bigham, J.M., Schwertmann, Udo, and Pfab, G., 1996, Influence of pH on mineral speciation in a bioreactor simulating acid mine drainage: Applied Geochemistry, v. 11, p. 845–849.

Bigham, J.M., Schwertmann, Udo, Traina, S.J., Winland, R.L., and Wolf, M., 1996, Schwertmannite and the chemical modeling of iron in acid sulfate waters: Geochimica et Cosmochimica Acta, v. 60, p. 2111–2121.

Blair, R.W., Yager, D.B., and Church, S.E., 2002, Surficial geologic maps along the riparian zone of the Animas River and its headwater tributaries, Silverton to Durango, Colorado, with upper Animas River watershed gradient profiles: U.S. Geological Survey Digital Data Series DDS–71.

Bove, D.J., Hon, Ken, Budding, K.E., Slack, J.F., Snee, L.W., and Yeoman, R.A., 2001, Geochronology and geology of late Oligocene through Miocene volcanism and mineralization in the western San Juan Mountains, Colorado: U.S. Geological Survey Professional Paper 1642, 30 p.

Briggs, P.H., and Fey, D.L., 1996, Twenty-four elements in natural and acid mine waters by inductively coupled plasma-atomic emission spectrometry, *in* Arbogast, B.F., ed., Analytical methods manual for the Mineral Resources Surveys Program: U.S. Geological Survey Open-File Report 96–525, p. 95–101.

Carlson, L., Bigham, J.M., Schwertmann, Udo, Kyek, A., and Wagner, F., 2002, Scavenging of As from acid mine drainage by schwertmannite and ferrihydrite—A comparison with synthetic analogues: Environmental Science and Technology, v. 36, no. 8, p. 1712–1719.

Carpenter, R.H., and Hayes, W.B., 1980, Annual accretion of Fe-Mn oxides and certain associated metals in a stream environment: Chemical Geology, v. 29, p. 249–259.

Casadevall, Thomas, and Ohmoto, Hiroshi, 1977, Sunnyside Mine, Eureka Mining District, San Juan County, Colorado—Geochemistry of gold and base metal ore deposition in a volcanic environment: Economic Geology, v. 72, p. 1285–1320.

d'Angelo, W.M., and Ficklin, W.H., 1996, Fluoride, chloride, nitrate, and sulfate in aqueous solution by chemically suppressed ion chromatography, *in* Arbogast, B.F., ed., Analytical methods manual for the Mineral Resources Surveys Program: U.S. Geological Survey Open-File Report 96–525, p. 149–153.

Desborough, G.A., Leinz, Reinhard, Sutley, Stephen, Briggs, P.H., Swayze, G.A., Smith, K.S., and Breit, George, 2000, Leaching studies of schwertmannite-rich precipitates from the Animas River headwaters, Colorado and Boulder River headwaters, Montana: U.S. Geological Survey Open-File Report 00–004, 16 p.

Desborough, G.A., and Yager, D.B., 2000, Acid-neutralizing potential of igneous bedrocks in the Animas River headwaters, San Juan County, Colorado: U.S. Geological Survey Open-File Report 00–165, 14 p.

Dzombak, D.A., and Morel, F.M.M., 1987, Adsorbtion of inorganic pollutants in aquatic systems: Journal of Hydraulic Engineering, v. 113, p. 430–475.

Dzombak, D.A., and Morel, F.M.M., 1990, Surface complexation modeling: New York, Wiley Interscience, 363 p.

Furniss, G., and Hinman, N.W., 1998, Ferricrete provides record of natural acid drainage, New World District, Montana: Water-Rock Interaction, Rotterdam, Balkema, p. 973–976.

Furniss, G., Hinman, N.W., Doyle, G.A., and Runnells, D.D., 1999, Radiocarbon-dated ferricrete provides a record of natural acid rock drainage and paleoclimatic changes: Environmental Geology, v. 37, p. 102–106.

Goddard, E.N., and others, 1948, Rock-color chart: Washington, D.C., National Research Council, 6 p. (Republished by Geological Society of America, 1951; reprinted, 1963, 1970, 1975.)

Hanshaw, Bruce, 1974, Geochemical evolution of a goethite deposit, 1st International Symposium on Water-Rock Interactions, Prague: p. 70–75.

Hach Company, 1992, Water analysis handbook: Loveland, Colo., Hach Company, p. 342–346.

Harder, E.M., 1915, Iron bacteria: Science, p. 310–311.

Hem, J.D., 1963, Chemical equilibria and rates of manganese oxidation: U.S. Geological Survey Water-Supply Paper 1667–A, 64 p.

Hem, J.D., 1964, Deposition and solution of manganese oxides: U.S. Geological Survey Water-Supply Paper 1667–B, 42 p.

Hem, J.D., 1977, Reactions of metal ions at surfaces of hydrous iron oxide: Geochimica et Cosmochimica Acta, v. 41, p. 527–538.

Hem, J.D., 1992, Study and interpretation of the chemical characteristics of natural water: U.S. Geological Survey Water-Supply Paper 2254, p. 84–89.

Jenne, E.A., 1968, Controls on Mn, Fe, Co, Ni, Cu, and Zn concentrations in soils and water—The significant role of hydrous Mn and Fe oxides: Advances in Chemistry, Series 73, p. 337–387.

Jenne, E.A., 1975, Trace element sorption by sediments and soils—Sites and processes, *in* Chappel, W., and Peterson, K., eds., Symposium on molybdenum in the environment, Volume 2: New York, M. Dekker, Inc., p. 425–553.

Kleinman, R.L.P., Crerar, D.A., and Pacelli, R.R., 1981, Biogeochemistry of acid mine drainage and a method to control acid formation: Mining Engineering, v. 33, p. 300–306.

Lamothe, P.J., Meier, A.L., and Wilson, S.A., 1999, The determination of forty-four elements in aqueous samples by Inductively Coupled Plasma–Mass Spectrometry: U.S. Geological Survey Open-File Report 99–151, 14 p.

Leib, K.J., Mast, M.A., and Wright, W.G., 2003, Using water-quality profiles to characterize seasonal water quality and loading in the upper Animas River basin, southwestern Colorado: U.S. Geological Survey Water-Resources Investigations Report 02–4230, 43 p.

Lind, C.J., and Hem, J.D., 1993, Manganese minerals and associated fine particulates in the streambed of Pinal Creek, Arizona, U.S.A.—A mining-related acid drainage problem: Applied Geochemistry, v. 8, p. 67–80.

Lovering, T.S., 1929, The New World or Cooke City Mining District, Park County, Montana: U.S. Geological Survey Bulletin 911–A, 87 p.

McKnight, D.M., Kimball, B.A., and Bencala, K.E., 1988, Iron photoreduction and oxidation in an acidic mountain stream: Science, v. 240, p. 637–240.

Miller, W.R., and McHugh, J.B., 1994, Natural acid drainage from altered areas within and adjacent to the Upper Alamosa River Basin, Colorado: U.S. Geological Survey Open-File Report 94–144, 47 p.

Miller, W.R., Bassett, R.L., McHugh, J.B., and Ficklin, W.H., 1999, The behavior of trace metals in water during natural acid sulfate weathering in an alpine watershed, *in* Plumlee, G.S., and Filipek, Lori, eds., The environmental geochemistry of mineral deposits—Part B, Case studies and research topics: Reviews in Economic Geology, v. 6B, p. 493–503.

Parkhurst, D.L., and Appelo, C.A.J., 1999, User's guide to PHREEQC (Version 2)—A computer program for speciation, batch-reaction, one-dimensional transport, and inverse geochemical calculations: U.S. Geological Survey Water-Resources Investigations Report 99–4259, 312 p.

Pierce, M.L., and Moore, C.B., 1980, Adsorption of arsenite on amorphous iron hydroxide from dilute aqueous solution: Environmental Science and Technology, v. 14, p. 214–216.

Ransome, F.L., 1901, A report on the economic geology of the Silverton quadrangle, Colorado: U.S. Geological Survey Bulletin 182, 265 p.

Robinson, G.D., 1993, Major-element chemistry and micromorphology of Mn-oxide coatings on stream alluvium: Applied Geochemistry, v. 8, p. 633–642.

Stollenwerk, K.G., 1994, Geochemical interactions between constituents in acidic groundwater and alluvium in an aquifer near Globe, Arizona: Applied Geochemistry, v. 9, p. 353–369.

Stookey, L.L., 1970, FerroZine—A new spectrophotometric reagent for iron: Analytical Chemistry, v. 42, p. 779–781.

Theobald, P.K., Lakin, H.W., and Hawkins, D.B., 1963, The precipitation of aluminum, iron, and manganese at the junction of Deer Creek with the Snake River in Summit County, Colorado: Geochimica et Cosmochimica Acta, v. 27, p. 121–132.

To, B.T., Nordstrom, D.K., Cunningham, K.M., Ball, J.W., and McCleskey, R.B., 1999, New method for direct determination of dissolved Fe(III) concentrations in acid mine waters: Environmental Science and Technology, v. 33, p. 807–813.

Wirt, Laurie, Leib, K.J., Bove, Dana, and Melick, Roger, 2001, Metal loading assessment of point and non-point sources in a small alpine sub-basin characterized by acid drainage—Prospect Gulch, upper Animas River watershed, Colorado: U.S. Geological Survey Open-File Report 01–0258, 36 p.

Wirt, Laurie, Leib, K.J., Mast, M.A., 2000, Chemical-constituent loads during thunderstorm runoff in a high-altitude alpine stream affected by acid drainage, *in* ICARD 2000*;* Proceedings of the Fifth International Conference on Acid Rock Drainage, Volume 2: Society for Mining, Metallurgy, and Exploration, Inc., p. 1391–1401.

Yager, D.B., Mast, M.A., Verplanck, P.L., Bove, D.J., Wright, W.G., and Hageman, P.L., 2000, Natural versus mining-related water quality degradation to tributaries draining Mount Moly, Silverton, Colorado, *in* ICARD 2000*;* Proceedings of the Fifth International Conference on Acid Rock Drainage, Volume 1: Society for Mining, Metallurgy, and Exploration, Inc., p. 535–547.

Yu, Jae-Young, Heo, Bong, Choi, In-Choi, Cho, Jeong-Pil, and Chang, Ho-Wan, 1999, Apparent solubilities of schwertmannite and ferrihydrite in natural stream waters polluted by mine drainage: Geochimica et Cosmochimica Acta, v. 63, p. 3407–3416.